International Journal of Heat and Mass Transfer 66 (2013) 553–574

Contents lists available at ScienceDirect

International Journal of Heat and Mass Transfer

journal homepage: www.elsevier.com/locate/ijhmt

Heat transfer correlation for flow boiling in small to micro tubes

Mohamed M. Mahmoud [a], Tassos G. Karayiannis [b,*]

[a] Faculty of Engineering, Zagazig University, POT44519, Egypt
[b] School of Engineering and Design, Brunel University London, Uxbridge, Middlesex UB8 3PH, UK

ARTICLE INFO

Article history:
Received 6 November 2012
Received in revised form 14 July 2013
Accepted 15 July 2013
Available online 15 August 2013

Keywords:
Flow boiling
Correlations
Models
Microtubes

ABSTRACT

There is a large discrepancy in the open literature about the comparative performance of the existing macro and microscale heat transfer models and correlations when applied to small/micro flow boiling systems. This paper presents a detailed comparison of the flow boiling heat transfer coefficient for R134a in stainless steel micro tubes with 21 macro and microscale correlations and models. The experimental database that was used in the comparison includes the data for 1.1 and 0.52 mm diameter tubes, mass flux range of 100–500 kg/m^2 s and system pressure range 6–10 bar obtained in the course of this study. The effect of the evaporator heated length on the comparative performance of the correlations and models was investigated using three different lengths of the 1.1 mm diameter tube (L = 150, 300 and 450 mm). This comparative study demonstrated that none of the assessed models and correlations could predict the experimental data with a reasonable accuracy. Also, the predictability of most correlations becomes worse as the heated length increases. This may contribute in explaining the discrepancy in the comparative performance of the correlations from one study to another. A new correlation is proposed in the present study based on the superposition model of Chen. The database used in developing the correlation consists of 5152 data points including the current experimental data and data obtained previously with the same test rig, fluid and methodology for tubes of diameter 4.26, 2.88, 2.01 mm. The new correlation predicted 92% of the data within the ±30% error bands with a MAE value of 14.3%.

1. Introduction

Micro evaporators are expected to play a vital role in the miniaturisation of cooling systems and required increase in energy efficient equipment. Therefore, they also have the potential of reducing capital cost and environmental problems such as global warming. Moreover, micro evaporators have several benefits over conventional ones. These include: (i) larger heat transfer surface area per unit volume; (ii) fewer number of flow patterns with well-defined liquid vapour interface which can allow the development of mechanistic models rather than empirical correlations; (iii) much higher flow boiling heat transfer coefficients; (v) smaller dependence on orientation due to the dominance of surface tension over buoyancy force. Despite these benefits, there is still a major limitation that may impede the development of these micro evaporators from the laboratory to commercial applications, i.e. the lack of reliable correlations to predict the flow boiling heat transfer coefficients at the microscale level. This is necessary for the correct design and operation of this kind of exchangers and their systems. Watel [1] reported that the current design advancement of compact heat exchangers is based on experience and experimentation on prototype units due to the lack of reliable prediction methods. Also, Ribatiski et al. [2] reported that micro evaporators are developed in a "heuristic way" without proven thermal design methods for predicting heat transfer and pressure drop.

Despite the more recent published correlations, the conclusion that there are still no reliable correlations for the prediction of the heat transfer coefficient, as stated above, is still valid. This lack of accurate prediction methods urged researchers to conduct more experimental studies on flow boiling heat transfer at microscale with the aim of developing new correlations or models. Accordingly, several microscale flow boiling heat transfer correlations were proposed by many authors. However, these correlations are not general and cannot be extrapolated outside their applicability ranges. For example, many researchers such as [3–10] assessed a large number of existing macro and microscale heat transfer correlations and reported poor agreement with experimental data. Bertsh et al. [11] performed an extensive review and comparative analysis of saturated flow boiling in microchannels. They assessed

* Corresponding author. Tel.: +44 (0) 1895 267132; fax: +44 (0) 1895 256392.
E-mail address: tassos.karayiannis@Brunel.ac.uk (T.G. Karayiannis).

0017-9310
http://dx.doi.org/10.1016/j.ijheatmasstransfer.2013.07.042

Nomenclature

Bd	bond number, $g\Delta\rho D^2/\sigma$, (–)
Bo	boiling number, q/Gh_{fg}, (–)
C	Chisholm constant, (–)
Co	confinement number, $(\sigma/g\Delta\rho)^{0.5}/D$
C_{pL}	liquid specific heat, (J/kg K)
D	diameter, (m)
D_b	bubble departure diameter, (m)
E	energy, (J)
F	convective boiling enhancement factor, (–)
F_{fl}	fluid dependant parameter, (–)
F_{nb}	nucleate boiling factor, (–)
f_{max}	maximum frequency, (s^{-1})
Fr	Froude number, V^2/gD, (–)
f	fanning friction factor, (–)
G	mass flux, (kg/m^2 s)
g	gravitational acceleration, (m/s^2)
h	heat transfer coefficient, (W/m^2 K)
h_{fg}	latent heat of vaporisation, (J/kg)
k	thermal conductivity, (W/m K)
L	length, (m)
M	molecular mass, (kg/kmol)
MAE	mean absolute error, (–)
N	number of data points
N_{Co}	convection number, $\left(\frac{1-x}{x}\right)^{0.8}\left(\frac{\rho_g}{\rho_L}\right)^{0.5}$, (–)
Nu	Nusselt number, (–)
P	pressure, (bar)
P_r	reduced pressure, $P/P_{critical}$, (–)
Pr	Prandtl number, (–)
q	heat flux, (W/m^2)
R_p	surface roughness, (m)
Re_{Lo}	all-liquid Reynolds number, GD/μ_L, (–)
Re_L	liquid Reynolds number, $(1-x)GD/\mu_L$, (–)
Re_{tp}	two-phase Reynolds number = $Re_L F^{1.25}$, (–)
S	nucleate boiling suppression factor, (–)
t	time, (s)
t_{dry}	time for dry vapour to pass a fixed location, (s)
t_{film}	residence time for liquid film, (s)
T	temperature, (K)
V	velocity, (m/s)
We	Weber number, $G^2D/\rho\sigma$, (–)
x	vapour quality, (–)
X	Martinelli parameter, $X=\left(\frac{f_L}{f_g}\right)^{0.5}\left(\frac{\rho_g}{\rho_L}\right)^{0.5}\left(\frac{1-x}{x}\right)$ (–)
Z	axial distance, (m)

Greek symbols

β	percentage of data within ±30%
δ	film thickness, (m)
δ_0	initial film thickness, (m)
ΔT	temperature difference, (K)
μ	viscosity, (Pa s)
ρ	density, (kg/m^3)
σ	surface tension, (N/m)
ϕ	two phase frictional multiplier, $\phi^2 = 1 + \frac{C}{X} + \frac{1}{X^2}$ (–)
τ	time, s or shear stress, (N/m^2)
τ_b	bubble generation period, (s^{-1})

Subscripts

a	annular
c	coalescence
CBD	convective boiling dominated
EXP,i	experimental data point number i
fg	liquid to gas phase change
g	gas
go	all-gass
h	hydraulic
L	liquid
Lo	all-Liquid
NBD	nucleate boiling dominated
nb	nucleate boiling
Pred, i	predicted data point number i
sp,lam	single phase laminar
tp	two phase
vv	laminar–laminar
tt	turbulent–turbulent
vt	laminar–turbulent
tv	turbulent–laminar
0	reference value

25 correlations using 1847 data points collected from 10 different laboratories, including 19 correlations developed for small to micro diameter channels. They concluded that the best prediction achieved had a mean absolute percentage error (MAE) value of 40% with less than 50% of the data within the ±30% error bands. This led them to conclude that, microscale heat transfer correlations did not add any advantages over conventional ones. Also, correlations that were developed based on fitting the experimental data failed upon extrapolation to predict other data points, while nucleate pool boiling correlations were better, indicating the possible dominance of nucleate boiling in microchannels. Finally, they confirmed the need for physics-based models for predicting the flow boiling heat transfer coefficient in microchannels. In addition to the non generality of macro and microscale correlations, there is a large discrepancy in the open literature about the comparative performance of these correlations when applied at microscale level. For example, the correlation of Lee and Lee [12], which was developed based on R113, predicted the experimental data of Wang et al. [10] for ethanol very well with a MAE value of 16.4%. On the contrary, the same correlation predicted poorly the experimental data of Qu and Mudawar [13] for de-ionised water with a MAE value of 272.1%. In fact, the discrepancy about the comparative performance of flow boiling heat transfer correlations is consistent with the discrepancy about the published heat transfer results from one study to another. Yet, the reasons behind this large scatter in the published heat transfer results are not clear. Karayiannis et al. [14] proposed two possible reasons for this discrepancy, i.e. the variations in the test section surface finish and heated length. They experimentally investigated the effect of these two parameters on the local behaviour of flow boiling heat transfer coefficient of R134a in micro stainless steel tubes.

Following on from the discussion above, this study presents an extensive assessment of 21 macro and microscale correlations and models. The assessment is conducted using local (h vs. x) and average global values (local and global comparison) using an experimental database for refrigerant R134a, D = 0.52 mm (L = 100 mm), D = 1.1 mm (L = 150, 300, 450 mm), G = 100–500 kg/m^2 s and P = 6–10 bar. This database includes the effect of heated length on the comparative performance of the examined correlations and models. Additionally, a new correlation of the Chen type is proposed based on the current database as well as previously obtained data using the same test rig for tubes with

Table A1
Existing microscale heat transfer correlations.

Reference	Correlation	Applicability range
Lazarek and Black [27]	$h_{tp} = 30\mathrm{Re}_{Lo}^{0.857} Bo^{0.714}(k_L/D)$	Based on 728 data points D = 3.1 mm G = 125–750 kg/m^2 s q = 14–380 kW/m^2 P = 1.3–4.1 bar R113
Tran et al. [28]	$h_{tp} = 840000(Bo^2 We_L)^{0.3}\left(\frac{\rho_L}{\rho_g}\right)^{-0.4}\ We_L = \frac{G^2 D}{\rho_L \sigma}$	D = 2.4, 2.92 mm, G = 44–832 kg/m^2 s q = 7.5–129 kW/m^2 P_r = 0.045–0.2 R12, R113
Kew and Cornwell [22]	$h_{tp} = 30\mathrm{Re}_{Lo}^{0.857} Bo^{0.714}\frac{k_L}{D}(1-x)^{-0.143}$	R141b, D = 1.39–3.69 mm
Warrier et al. [4]	$h_{tp} = [1 + 6Bo^{1/16} - 5.3x^{0.65}(1 - 855Bo)]\frac{4.36k_L}{D}$	$0.00027 \leqslant Bo \leqslant 0.000890.03 \leqslant x \leqslant 0.55$ FC84, D_h = 0.75 mm
Kandlikar and Balasubramanian [23]	$h_{tp} = \max(h_{CBD}, h_{NBD})\ (1-x)^{0.8} h_{Lo}$	Range of data for the original Kandlikar [25] correlation
	$h_{NBD} = (0.6683 N_{Co}^{-0.2} + 1058\, Bo^{0.7} F_{Fl})\ h_{CBD} = 1.136 N_{Co}^{-0.9} + 667.2 Bo^{0.7} F_{Fl}$	D = 0.19–32.0 mm
		G = 13–8179 kg/m^2 s
	$N_{Co} = \left(\frac{1-x}{x}\right)^{0.8}\left(\frac{\rho_g}{\rho_L}\right)^{0.5}$	q = 0.3–2280 kW/m^2
	$h_{\mathrm{Lo}} = \frac{\mathrm{Re}_{Lo}\mathrm{Pr}_L(f/2)(k_L/D)}{1+12.7(\mathrm{Pr}_L^{2/3}-1)(f/2)^{0.5}},\ 10^4 \leqslant \mathrm{Re}_{\mathrm{Lo}} \leqslant 5\times 10^6$	P = 0.4–64 bar
	$h_{\mathrm{Lo}} = \frac{(\mathrm{Re}_{Lo}-1000)\mathrm{Pr}_L(f/2)(k_L/D)}{1+12.7(\mathrm{Pr}_L^{2/3}-1)(f/2)^{0.5}},\ 3\times 10^3 \leqslant \mathrm{Re}_{\mathrm{Lo}} \leqslant 10^4$	Water, refrigerants
	For 1600 < Re_{Lo} < 3000), h_{Lo} is calculated by interpolation between Re_{Lo} = 1600 and 3000	
	For Re_{Lo} < 1600, h_{Lo} is calculated from Nu = constant	
	For $Re_{Lo} \leqslant 100$, $h_{tp} = h_{NBD}(1-x)^{0.8} h_{Lo}$	
Zhang et al.[16]	$h_{tp} = Sh_{nb} + Fh_L$	D = 0.78–6.0 mm
	$h_{nb} = 0.00122\left(\frac{k_L^{0.79} C_{pL}^{0.45}\rho_L^{0.49}}{\sigma^{0.5}\mu_L^{0.29} h_{fg}^{0.24}\rho_g^{0.24}}\right)\Delta T_{sat}^{0.24}\Delta P_{sat}^{0.75}$	G = 23.4–2939 kg/m^2 s
	$S = (1 + 2.53\times 10^{-6}\mathrm{Re}_L^{1.17})^{-1}$	q = 2.95–2511 kW/m^2
	$F = MAX(F', 1)$, $F' = 0.64\phi_L$	P = 1.01–8.66 bar
	$\phi_L^2 = 1 + \frac{C}{X} + \frac{1}{X^2}$	Water, refrigerants
	for Re_L < 1000 and Re_g < 1000 $X = X_{vv}$ and C = 5	
	for Re_L > 2000 and Re_g < 1000 $X = X_{tv}$ and C = 10	
	for Re_L < 1000 and Re_g > 2000 $X = X_{vt}$ and C = 12	
	for Re_L > 2000 and Re_g > 2000 $X = X_{tt}$ and C = 20	
	For other regions of Re_k ($k = L$ or g) interpolate the above values of C	
	$X = \left[\left(\frac{dP}{dz}\right)_L / \left(\frac{dP}{dz}\right)_g\right]^{0.5} = \left(\frac{f_L}{f_g}\right)^{0.5}\left(\frac{1-x}{x}\right)\left(\frac{\rho_g}{\rho_L}\right)^{0.5}$	
	$f_{L \text{ or } g} = \begin{cases} 16/\mathrm{Re}_{L\,\mathrm{or}\,g}, & \text{for tubes, } \mathrm{Re}_{L\,\mathrm{or}\,g} < 1000 \\ 0.046\,\mathrm{Re}_{L\,\mathrm{or}\,g}^{-0.2}, & \mathrm{Re}_{L\,\mathrm{or}\,g} > 2000 \end{cases}$	
	$h_L = (k_L/D)Nu$	
	$Nu = \begin{cases} \max(4.36, Nu_{Collier}), & \text{for } \mathrm{Re}_L \leqslant 2000 \\ 0.023\mathrm{Re}_L^{0.8}\mathrm{Pr}_L^{0.4}, & \text{for } \mathrm{Re}_L \geqslant 2300 \end{cases}$	
	$Nu_{Collier} = 0.17\mathrm{Re}_L^{0.33}\mathrm{Pr}_L^{0.43}\left(\frac{\mathrm{Pr}_L}{\mathrm{Pr}_w}\right)^{0.25} \times \left[\frac{g\beta\rho_L^2 D_h^3(T_w - T_L)}{\mu_L^2}\right]^{0.1}$	
Lee and Mudawar [29]	For $0 < x \leqslant 0.05$ $h_{tp} = 3.856X^{0.267}h_L$	Water, R134a D_h = 0.35 mm
	For $0.05 < x \leqslant 0.55$ $h_{tp} = 436.48Bo^{0.522}We_L^{0.351}X^{0.665}h_L$	
	For $0.55 < x \leqslant 1$ $h_{tp} = MAX(108.6X^{1.665}h_g, h_g)$	
Saitoh et al. [17]	$h_{tp} = Sh_{nb} + Fh_L$	D = 0.5–11 mm
	$h_{nb} = 207\frac{k_L}{D_b}\left(\frac{qD_b}{k_L T_L}\right)^{0.745}\left(\frac{\rho_g}{\rho_L}\right)^{0.581}\mathrm{Pr}_L^{0.533}$	G = 150–450 kg/m^2 s
	$D_b = 0.512[\sigma/g(\rho_L - \rho_g)]^{0.5}$	q = 5–39 kW/m^2
	$F = 1 + \left(\frac{1}{X}\right)^{1.05}/(1 + We_g^{-0.4})$	P = 3.5–5 bar
	$S = 1/(1 + 0.4(F^{1.25}\times \mathrm{Re_L}\times 10^{-4})^{1.4})$	R134a
	$h_L = \begin{cases} 0.023\frac{k_L}{D}\mathrm{Re}_L^{0.8}\mathrm{Pr}_L^{1/3} & \mathrm{Re_L} \geqslant 1000 \\ \frac{4.36k_L}{D} & \mathrm{Re_L} < 1000 \end{cases}$	
	$X = \left(\frac{1-x}{x}\right)^{0.9}\left(\frac{\rho_g}{\rho_L}\right)^{0.5}\left(\frac{\mu_L}{\mu_g}\right)^{0.1}$ for $\mathrm{Re_L} > 1000\ \&\ \mathrm{Re_g} > 1000$	
	$X = \left(\frac{f_L}{f_g}\right)^{0.5}(\mathrm{Re}_g^{-0.4})\left(\frac{G_L}{G_g}\right)^{0.5}\left(\frac{\rho_g}{\rho_L}\right)^{0.5}\left(\frac{\mu_L}{\mu_g}\right)^{0.5}$ for $\mathrm{Re_L} < 1000\ \&\ \mathrm{Re_g} > 1000$	
Bertsch et al. [18]	$h_{tp} = Sh_{nb} + Fh_{conv}$ $S = (1-x)$	3899 data points
	$h_{np} = 55P_r^{0.12-0.434\ln R_p}(-\log P_r)^{-0.55}M^{-0.5}q^{0.67}$	D = 0.16–2.92 mm
	$h_{conv} = (1-x)h_{Lo} + xh_{go}$	Co = 0.3–4
	For turbulent flow h_{Lo} and h_{go} are calculated from the Dittus–Boelter equation	G = 20–3000 kg/m^2 s
	For laminar flow:	x = 0–1
	$h_{Lo/go} = \frac{k_{L/g}}{D}\left[3.66 + \frac{0.0668\frac{D}{L}\mathrm{Re}_{Lo/go}\mathrm{Pr}_{L/g}}{1+0.04(D\mathrm{Re}_{Lo/go}\frac{\mathrm{Pr}_{L/g}}{L})^{2/3}}\right]$	12 fluids including cryogens and refrigerants
	$F = 1 + 80(x^2 - x^6)\exp(-0.6Co)$	
	$Co = \lVert\sigma/g\Delta\rho\rVert^{0.5}/D$	
Mikielewicz [24]	$\frac{h_{tp}}{h_{Lo}} = \sqrt{\phi_{MS}^n + \frac{1}{1+P}\left(\frac{h_{nb}}{h_{Lo}}\right)^2}$	Applicable for conventional and small diameter channels
	$P = 0.00253\mathrm{Re}_{Lo}^{1.17}Bo^{0.6}(\phi_{MS} - 1)^{-0.65}$	
	$\phi_{MS} = \left[1 + 2\left(\frac{1}{f_1} - 1\right)xCo^{-1}\right](1-x)^{1/3} + \frac{x^3}{f_2}$	
	For laminar flow	

(continued on next page)

Table A1 (*continued*)

Reference	Correlation	Applicability range
	$f_1 = \frac{\rho_g}{\rho_L}\frac{\mu_L}{\mu_g}$	
	$f_2 = \frac{\mu_g}{\mu_L}\frac{c_{pL}}{c_{pg}}\left(\frac{k_L}{k_g}\right)^{1.5}$	
	For turbulent flow:	
	$f_1 = \frac{\rho_g}{\rho_L}\left(\frac{\mu_L}{\mu_g}\right)^{0.25}$	
	$f_2 = \left(\frac{k_g}{k_L}\right)$	
	$h_{np} = 55P_r^{0.12-0.434\ln R_p}(-\log P_r)^{-0.55}M^{-0.5}q^{0.67}$	
Li and Wu [30]	$h_{tp} = 334Bo^{0.3}(Bd\mathrm{Re}_L^{0.36})^{0.4}\frac{k_L}{D}$	769 data points D = 0.148–3.25 mm 12 different fluids
Mohamed and Karayiannis [31]	For D = 4.26–1.1 mm	5152 data points
	$h_{tp} = 3320\frac{Bo^{0.63}We_L^{0.2}\mathrm{Re}_L^{0.11}}{Co^{0.6}}\frac{k_L}{D}$	D = 4.26–0.52 mm
	For D = 0.52 mm, $x \leqslant 0.3$	G = 100–500 kg/m^2 s
	$h_{tp} = 3320\frac{Bo^{0.63}We_L^{0.2}\mathrm{Re}_L^{0.11}}{Co^{0.6}}\frac{k_L}{D}$	q = 2.4–175.4 kW/m^2
	For D = 0.52 mm, $x > 0.3$	P = 6–14 bar
	$h_{tp} = 5324\left[\frac{Bo^{0.3}We_L^{0.25}}{N_{Co}^{0.25}}\right]^{1.79}\frac{k_L}{D}$	

inner diameters of 4.26, 2.88 and 2.01 mm and the same refrigerant.

2. Microscale heat transfer prediction methodS

2.1. Empirical correlations

Nucleate and convective boiling mechanisms contribute to the flow boiling heat transfer process. Thus, the flow boiling heat transfer correlations should consider, through a certain approach, the contribution of the two mechanisms. The review of the previous studies demonstrated that three approaches were commonly adopted. The first approach is the superposition model proposed by Chen [15] in which nucleate and convective boiling contributions were simply added together. Examples on this approach are the correlations proposed by Zhang et al. [16], Saitoh et al. [17] and Bertsch et al. [18], see Table A1. Zhang et al. [16] proposed a correlation for saturated flow boiling heat transfer in minichannels based on a database consisting of 1203 data points for four fluids (water, R11, R12 and R113), D = 0.78–6 mm, P = 0.101–1.21 MPa, G = 23.4–2939 kg/m^2 s and q = 2.95–2511 kW/m^2. Most of the data were in the laminar liquid-turbulent gas flow condition. They modified the convective boiling enhancement factor (F) in the original Chen correlation to be a function of the two phase frictional multiplier (ϕ_L) which depends on flow conditions (laminar/turbulent). In the original correlation, this factor was given as a function of the turbulent-turbulent Martinelli parameter (X_{tt}). Also, the single phase liquid heat transfer coefficient (h_L) was modified based on flow conditions instead of using the Dittus–Boelter correlation in the original correlation. All other terms in the Chen correlation were kept unchanged except the nucleate boiling suppression factor (S) where the two phase Reynolds number (Re_{tp}) in the original correlation was replaced with the liquid Reynolds number (Re_L). Despite these changes, this correlation predicted their database with a MAE value comparable to that predicted by the original Chen correlation, which was of the order of 21%. Saitoh et al. [17] proposed a correlation of the Chen type that takes into account the effect of channel diameter. The correlation was based on 2224 data points collected for R134a in horizontal tubes of diameters ranging from 0.51 to 11 mm. The effect of channel diameter was taken into consideration by incorporating the gas phase Weber number (We_g) into the convective boiling enhancement factor. The nucleate boiling suppression factor was modified based on the new enhancement factor, i.e. depends also on We_g. For the nucleate boiling part, they suggested using the nucleate pool boiling correlation of Stephan–Abdelsalam [19] that was developed for refrigerants rather than using the Forster–Zuber [20] correlation. Bertsch et al. [18] proposed a correlation for predicting the saturated flow boiling heat transfer coefficient in mini and microchannels. This correlation was developed based on a large experimental data base consisting of 3899 data points which were collected from 14 different experimental studies and included 12 different fluids including refrigerants and diameters ranging from 0.16 to 2.92 mm. The Cooper [21] correlation was recommended for the nucleate pool boiling term. The nucleate boiling suppression factor was found to be dependent on vapour quality only rather than the two phase Reynolds number. Thus they simply used the term $(1 - x)$ as a nucleate boiling suppression factor. The single phase heat transfer coefficient in the convective boiling term was calculated as the average of the all-liquid single phase heat transfer coefficient (h_{Lo}) and the all-vapour single phase heat transfer coefficient (h_{go}) weighed by vapour quality. They modified the convective boiling enhancement factor and correlated it as a function of vapour quality (x) and the confinement number (Co) proposed by Kew and Cornwell [22]. This correlation predicted their database with a MAE value of 28% and with more than 60% of the data located within ±30% error bands.

The second approach adopted in developing flow boiling heat transfer correlations was the asymptotic model in which the heat transfer coefficient approaches either the nucleate boiling or the convective boiling components, i.e. selecting the component which is the largest, as described in the work of Kandlikar and Balasubramanian [23] and Mikielewicz [24], see Table A1. Kandlikar and Balasubramanian [23] extended the macroscale correlation of Kandlikar [25] to incorporate transition and laminar patterns in microchannels. The original correlation of Kandlikar [25] assumed that the contribution of nucleate and convective boiling mechanisms is additive for each region, i.e. the nucleate boiling dominant region and the convective boiling dominant region. The total two phase heat transfer coefficient was selected as the largest of the heat transfer coefficients in the nucleate boiling and the convective boiling dominant region. The effect of fluid type was incorporated using a fluid dependent parameter (F_{fl}) in the nucleate boiling term. This parameter acted as a correction factor that accounts for all other parameters influencing nucleate boiling. The new microscale modifications include: (i) dropping the Froude number (Fr) from the original correlation because channel orientation is insignificant in mini/microchannels and (ii) modifying the single phase heat transfer coefficient based on flow conditions, i.e. laminar, transition and turbulent. The correlation is valid for water and refrigerants and for $D = 0.19–32.0$ mm, $G = 13–8179$ kg/m^2 s, $q = 0.3–2280$ kW/m^2, $P = 0.4–64$ bar. It was proposed that the single phase liquid heat transfer coefficient in the transition region can be calculated by interpolation between the all-liquid Reynolds number, $Re_{Lo} = 1600$ and $Re_{Lo} = 3000$. Mikielewicz [24] proposed a model based on the analogy between momentum transfer and energy transfer. The model started with the premise that the total energy dissipation in the flow is the sum of the energy dissipation due to shearing flow without nucleation and the energy dissipation due to nucleation. Under steady state conditions in two phase flow, the energy dissipation was approximated by the viscous energy dissipation per unit volume in the boundary layer. Using the analogy between momentum and energy transfer, the two phase heat transfer coefficient was written in a form similar to the asymptotic model with an exponent $n = 2$ but this exponent was obtained based on a theoretical analysis rather than empirical adjustments. The two phase heat transfer coefficient was expressed in terms of the frictional two phase multiplier of Műller-Steinhagen and Heck [26], the boiling number (Bo) and the all-liquid Reynolds number. The Cooper [21] pool boiling correlation was recommended for the nucleate boiling term corrected by a factor that depends on the all-liquid Reynolds number, boiling number and the frictional two phase multiplier.

In addition to the two complex approaches mentioned above, a third simple approach was followed by some researchers through fitting their experimental data as a function of the most important dimensionless groups, i.e. statistical correlations. Examples on this approach are the correlations proposed by researchers [27,28,22,4,29–31], see Table A1. Lazarek and Black [27] correlated their 728 data points by fitting the data using the least square method as a function of boiling number and the all-liquid Reynolds number. It is worth noting that the exponent of the Bo number in the correlation is almost similar to the exponent of heat flux in the nucleate pool boiling correlations. In other words, the correlation indicates the dominance of nucleate boiling and also takes into consideration the effect of tube diameter. Also, it is clear from the correlation that the mass flux effect is small, i.e. the exponent of the mass flux is 0.143. The correlation is valid for R113, $D = 3.1$ mm, $G = 125–750$ kg/m^2 s, $q = 14–380$ kW/m^2 and $P = 1.3–4.1$ bar. Tran et al. [28] investigated flow boiling heat transfer of R12 in a circular channel with diameter 2.46 mm and a rectangular channel with a hydraulic diameter of 2.4 mm. They found that nucleate boiling is the dominant mechanism and the mass flux effect was insignificant. Accordingly, they modified the correlation of Lazarek and Black [27] by replacing the all-liquid Reynolds number with the liquid Weber number and taking the effect of fluid type into account by incorporating the liquid to vapour density ratio. The Weber number was used to replace the viscous effects in favour of surface tension. The correlation indicates that there is no mass flux effect (the exponent of mass flux is zero) and the diameter effect is small, which is clear from the exponent of the Weber number. It is worth mentioning that the liquid Weber number is defined based on the total mass flux (G) and the correlation does not show any dependence on vapour quality. The correlation is valid for R12, R113, $D = 2.4$, 2.92 mm, $G = 44–832$ kg/m^2 s, $q = 7.5–129$ kW/m^2, $P_r = 0.045–0.2$. Kew and Cornwell [22] investigated flow boiling heat transfer of R141b in stainless steel tubes having inner diameters of 1.39–3.69 mm and heated length of 500 mm. The experimentally determined heat transfer coefficient in their study increased with increasing vapour quality towards the tube exit over a wide range of vapour quality values. Accordingly, they modified the Lazarek and Black [27] correlation by the term $(1 - x)^{-0.143}$ to account for the increasing trend of the heat transfer coefficient with quality. Warrier et al. [4] investigated flow boiling heat transfer of FC84 in aluminium multi-channels with a hydraulic diameter of 0.75 mm. They assessed two macroscale correlations, that of Kandlikar [25] and Liu and Winterton [32] and two microscale correlations proposed by Lazarek and Black [27] and Tran et al. [33]. All the examined correlations significantly overpredicted the experimental data but captured the experimental trend of the local heat transfer coefficient, which was independent of local quality. The only exception in their comparison was the correlation of Tran et al. [33] that predicted an incorrect trend, i.e. it showed a sharply decreasing trend with increasing quality. The behaviour of the Tran et al. [33] correlation reported in [14] was not consistent with the experimental results of Tran et al. which do not show any dependence on local quality. The incorrect trend of the Tran et al. correlation was resulting from the fact that the authors in [14] multiplied the confinement number by $(1 - x)$, which did not exist in the Tran et al. original heat transfer correlation but in the pressure drop correlation. Eventually, they correlated the two phase heat transfer coefficient normalised by the single phase laminar heat transfer coefficient as a function of boiling number and vapour quality. This correlation is valid for FC84, $D_h = 0.75$ mm, $0.00027 \leqslant Bo \leqslant 0.00089$ and $0.03 \leqslant x \leqslant 0.55$.

Lee and Mudawar [29] investigated flow boiling heat transfer of R134a in a microchannel heat sink with a hydraulic diameter of 0.35 mm. The macro and microscale correlations failed to predict their experimental data and thus they proposed a new correlation for saturated flow boiling in microchannels. The correlation was developed based on 318 data points of which 111 data points were for R134a and the remaining for water. They found that the boiling number and the liquid Weber number as well as the Martinelli parameter are the important dimensionless parameters to be included in the correlation. They divided the quality domain into three ranges based on the dominant mechanism in order to achieve accurate predictions and proposed a correlation for each range. In the first range ($x < 0.05$), the dominant mechanism was nucleate boiling whereas convective boiling dominated at the intermediate quality range ($x = 0.05–0.55$) and high quality range ($x > 0.55$). Although nucleate boiling was the prevailing mechanism at very low quality, the heat transfer coefficient was correlated as a function of the Martinelli parameter only, which is a flow parameter without including any term for the heat flux effect in this region. Li and Wu [30] collected a large number of experimental data points from the open literature covering saturated flow boiling heat transfer in mini/microchannels. The database consists of 3744 data points and covers hydraulic diameters ranging from 0.16 to 3.1 mm with most data located in the laminar regime. They have correlated the data as a function of three dimensionless parameters namely boiling number, Bond number (Bd) and liquid Reynolds number. The boiling number accounts for the heat and mass flux effects, the Reynolds number accounts for inertia and viscous effects and the Bond number accounts for gravity and surface tension effects. Mahmoud and Karayiannis [31] proposed very recently a statistical correlation for flow boiling heat transfer of R134a in micro tubes with diameter ranging from 4.26 to 0.52 mm. The heat transfer coefficient was fitted as a function of boiling number, Weber number, liquid Reynolds number, confinement number and convection number using the multi-parameter nonlinear least square fitting. The correlation was based on 5152 data points excluding dryout data and valid for $G = 100–500$ kg/m^2 s, $P = 6–14$ bar, $q = 2.4–175.4$ kW/m^2. This correlation predicted 91.4% of the data within the ±30% error bands with a MAE value of 15%.

2.2. Mechanistic models

The above review demonstrated that the developed microscale correlations are not general and may not be extrapolated with confidence outside their applicability ranges. Therefore, models based on the prevailing physical phenomena are also a way forward.

Unfortunately, there is a very limited number of mechanistic models in the open literature – and this reflects the lack of knowledge of the physical phenomena at the microscale level. Jacobi and Thome [34] proposed a heat transfer model based on the premise that thin-film evaporation into elongated bubbles is the most important mechanism in microchannels. At a fixed location, a pair composed of an elongated bubble and liquid slug was assumed to pass with a velocity equal to the homogeneous velocity. Principally, this model is based on the idea that during elongated bubble flow a thin liquid film of uniform thickness forms around the bubble and the film becomes thinner as evaporation starts until the arrival of the next liquid slug. This model requires the knowledge of the critical nucleation radius or effective wall superheat in order to estimate the frequency of the pairs and also requires the knowledge of the initial film thickness. When the model was compared with experimental data assuming initial film thickness in the order of 10–20 μm, it managed to predict the data, which confirmed that thin-film evaporation maybe the dominant mechanism in microchannels. Thome et al. [35] extended this model to include the passage of a vapour slug when dryout occurs and called it "three-zone model". In this version, a cyclic passage of liquid slug, elongated bubble and vapour slug was considered. The local time averaged heat transfer coefficient predicted by the model is given by Eq. (1). They got a continuous relation for the initial film thickness based on the work of Moriyama and Inoue [36] and applying the asymptotic approach. Dupont et al. [37] compared the model with a large experimental database collected from seven different studies and optimised the pair generation frequency, the final film thickness and the adjustable constant in the initial film thickness correlation. The database covered seven fluids namely: R11, R12, R113, R123, R134a, R141b and CO_2. The model successfully predicted 70% of the data within ±30% and the effects of various parameters such as heat flux, mass flux, system pressure and vapour quality.

$$h_{tp}(z) = \frac{t_L}{\tau_b} h_{Lo}(z) + \frac{t_{film}}{\tau_b} h_{film}(z) + \frac{t_{dry}}{\tau_b} h_{go}(z) \tag{1}$$

Shiferaw et al. [38] compared their experimental results for R134a and a diameter of 1.1 mm with the three-zone model. They reported that the model predicted fairly well data that could be interpreted traditionally in the nucleate boiling regime. The model over-predicted data in which dryout was thought to occur. The effect of pressure changes was correctly predicted but the actual experimental changes were greater. The model showed a slight effect of mass flux that was not seen in the data. The study included a parametric sensitivity of the model, which, according to Shiferaw et al. [38] could be useful for suggestions for modifications for improving the predictive capability of the model.

Qu and Mudawar [39] developed a mechanistic heat transfer model for the annular flow pattern region in microchannels. The model took into account the liquid droplet entrainment to the vapour core. They proposed a correlation for the mass transfer coefficient and applied the one dimensional mass and momentum conservation equations to obtain local parameters such as pressure gradient, film thickness, interfacial shear stress and flow rate in the liquid film. The two phase heat transfer coefficient was calculated by dividing the liquid thermal conductivity by the determined film thickness (k_L/δ). This model predicted all their experimental data for water with an uncertainty of ±40% and average error of 13.3%. Boye et al. [40] presented a one dimensional, steady state and incompressible flow model with constant properties for annular flow in microchannels. They applied the momentum equation for the liquid and vapour phases and obtained an analytical expression for the variation of the vapour core radius (film thickness) as a function of quality. The local heat transfer coefficient was then calculated from the local film thickness $h_{tp}(z) = k_L/\delta(z)$. Consolini and Thome [41] developed recently a heat transfer thin film evaporation model that takes bubble coalescence into consideration. The model is valid in the quality range from the transitional quality from isolated bubbles to coalescing bubble and the transition quality from coalescing to annular flow. This was to account for the redistribution of the liquid in the flow structure resulting from the breakup of liquid slugs during coalescence. They got an analytical expression for the average heat transfer coefficient as given by Eq. (2). A comparison of the model against their experimental data (980 data points) indicated that 83% of the data were predicted within the ±30% error band.

$$h_{tp}(x) = \frac{k_L}{D} \frac{\left(\frac{\rho_L}{\rho_g}\right)\left[\left(\frac{x_a - x}{x_a - x_c}\right)^{\beta}\right]^{\gamma} \ln\left(\frac{1-\theta_{1C}}{1-\theta_{2C}}\right)}{Bo(1-\psi_C)} \tag{2}$$

where: $\gamma = \left(\frac{x_a - x}{x_a - x_c}\right)^3$, $\beta = 1$, $Bo = \frac{q}{\rho_g h_{fg} D f_{\max}}$, $\psi_C = 0.002\beta\left(\frac{1-x_C}{x_a - x_C}\right)$

$$\theta_{1C} = \frac{(1-\psi_C)\ln^2\left(1 + \frac{\rho_L}{\rho_g}x_c\right)}{\theta_{3C}},$$

$$\theta_{2C} = \frac{(1-\psi_C)\left[\ln\left(1 + \frac{\rho_L}{\rho_g}x_c\right) + 4Bo\right]^2}{\theta_{3C}},$$

$$\theta_{3C} = 8\frac{\mu_L}{\tau_i}\frac{G}{\rho_g D}\frac{\rho_L}{\rho_g}x_c - \psi_C \ln^2\left(1 + \frac{\rho_L}{\rho_g}x_c\right)$$

$$\tau_i = (f_q + f_{v,Blasius})\frac{G^2 x_c^2}{2\rho_v},$$

$$f_q = 304\left(\frac{GD}{\mu_L}\right)^{-1.16}\left(\frac{\rho_L}{\rho_g}\right)^{-1.74}\left(\frac{\mu_L}{\mu_g}\right)^{1.43} x_c^{-2}\left[1 - \exp\left(-\frac{qD}{h_{fg}\mu_L}\right)\right]$$

$$f_{\max} = 0.004\left(\frac{q}{\sigma}\right)\left(\frac{\sigma^3}{q^2 D^3 \rho_g}\right) \quad x_c = 0.763\left(\frac{q\rho_g\sigma}{\mu_L h_{fg} G^2}\right)^{0.39}$$

$$x_a = 1.4\times10^{-4}\left(\frac{GD}{\mu_L}\right)^{1.47}\left(\frac{G^2 D}{\rho_L \sigma}\right)^{-1.23}$$

3. Experimental facility

An experimental facility was designed and constructed to investigate flow boiling of R134a in small to micro diameter tubes. The detailed description of the test rig can be found in earlier publications, [14,38,42]. Four stainless steel tubes were investigated in the current study: one tube with D = 0.52 mm and L = 100 mm and three tubes with D = 1.1 mm and L = 150, 300, 450 mm. All tubes are seamless cold drawn tubes made of stainless steel AISI316. Each test section consists of an adiabatic calming section with length of 150 mm, heated section and a borosilicate visualisation section with length of 100 mm. The heated section was directly heated by passing a DC current through two copper electrodes that were welded at the inlet and outlet. The power supplied was measured directly between the test section electrodes using a Yokogawa power meter WT110 with an accuracy of ±0.29%. This excluded the voltage drop across the connections between the power supply and the test section electrodes. The outer tube surface temperature was measured locally by K-type thermocouples with a mean absolute error of ±0.22 K attached at equal intervals. The first and last thermocouples were located away from the electrodes to avoid the effect of end heat losses at the electrodes. All thermocouples were attached to the surface by using an electrically insulating but thermally conducting epoxy. Fluid temperature and pressure were measured at the test section inlet and outlet using T-type thermocouples with accuracy of ±0.1 K and pressure transducers with accuracy of ±0.32% respectively. The pressure drop was directly measured between the test section inlet and outlet using a differential pressure transducer (PX771A-025DI) with an accuracy of ±0.1%. It is worth noting that, there are no flow restrictions at the test section inlet and outlet. A Phantom V4 digital high speed camera with 1000 frame/s and a resolution of 512×512 pixels was used for flow visualisation. The data were monitored through a Labview program at a frequency of 1 Hz using three data loggers: Solartron models SI35951E (two) and SI35351C. All the data were recorded for 90 s after attaining steady state and the sample of the 90 data points was averaged and used in the calculations. It is worth mentioning that the data used in this analysis correspond to stable boiling, see Karayiannis et al. [14] and Mahmoud et al. [43].The procedure used for calculating the heat transfer coefficient from the collected data is given in Mahmoud et al. [44]. The mean uncertainty in the heat transfer coefficient is 7.4%, see [44].

4. Assessment of correlations

This section presents a detailed assessment for six macroscale correlations [15,25,32,45–47] and twelve microcale correlations [4,16–18,22–24,27–31], see Tables A1 and A2 for the equations. In addition to that, Cooper [21] pool boiling correlation was assessed as a base case for pure nucleate boiling. The current experimental database included in the assessment consists of 5789 data points for R134a, for a tube with D = 0.52 mm and three tubes with D = 1.1 mm (L = 150, 300 and 450 mm) at P = 6–10 bar and G = 100–500 kg/m^2 s. It is worth mentioning that the data after dryout were excluded from the comparison because most correlations did not consider post dryout heat transfer. Dryout was identified, from the h vs. x graphs, as the local vapour quality at which the heat transfer coefficient starts to decrease rapidly. Table 1 summarizes the vapour quality range at which dryout occurred for each test section. The lower limit of the vapour quality range in Table 1 corresponds to $G > 200$ kg/m^2 s (the flow is turbulent or in the transition region) and the upper limit corresponds to $G \leqslant 200$ kg/m^2 s (laminar flow). A local (h vs. x) and global assessment was performed. The local assessment gives information on performance of the correlation compared to the experimental trend. The global assessment examines the validity of the correlation over a wide range of experimental conditions. The local assessment can also help explain the global performance of each correlation when it is compared with the experimental data. The widely used parameters for global assessment are the mean absolute percentage error (MAE) defined by Eq. (3) and the percentage of data (β) within ±30% error bands. N in Eq. (3) is the number of experimental data points.

$$\mathrm{MAE} = \frac{1}{N}\sum_{i=1}^{N}\frac{|h_{\mathrm{Pred},i} - h_{Exp,i}|}{h_{Exp,i}} \times 100 \tag{3}$$

4.1. Local assessment

Figs. 1 and 2 depict the local assessment of the examined macro and microscale correlations respectively. The correlations proposed by Lazarek and Black [27] and Tran et al. [28] were not included here since they correlated the average heat transfer coefficients without any dependence on local quality. The assessment was conducted at a mass flux value of 300 kg/m^2 s, system pressure of 6 bar and a selected value of heat flux. Since all examined correlations superimpose the contributions of nucleate and convective boiling mechanisms, the heat flux value was selected such that the corresponding exit quality is about 0.7–0.8 to cover nucleate and convective boiling regions if they exist. The ±30% error band is also shown in Figs. 1 and 2. It is worth mentioning that Figs. 1 and 2 do not represent all the complete data set (5789 data point). The aim of these figures was only to compare the experimental trend with that predicted by the correlation at a certain experimental condition. This trend comparison was to test the performance of each correlation over a wide range of vapour quality. It is obvious from Fig. 1(a), for the 0.52 mm tube, that all macroscale correlations failed to predict the correct experimental trend except the correlation of Shah [45]. It shows similar trend to the experiment but with values much lower than the experimental values. Both Shah [45] and Kandlikar [25] correlations show a change in the trend at $x \approx 0.1$ and $x \approx 0.4$, respectively while other correlations do not show this change. Stiener and Taborek [47] correlation highly over-predicts the experimental data and gives a heat transfer coefficient that is almost constant with local vapour quality. Gungor and Winterton [46] correlation gives heat transfer coefficient values that slightly decrease with increasing vapour quality. It is clear also that, there is no significant difference between Chen [15] and Liu and Winterton [32] correlations. Additionally, the difference between all correlations, except those of Gungor and Winterton [46] and Stiener and Taborek [47], becomes small as the vapour quality increases. The values predicted by Kandlikar [25] correlation are the closest to the experimental values but only over a narrow quality range $x \approx 0.1$–0.3.

Fig. 1(b) shows for D = 1.1 mm (L = 150 mm) that, Kandlikar [25] correlation gives excellent agreement with the experimental trend and magnitude of the heat transfer coefficient. Contrary to the comparison with the 0.52 mm diameter tube data, Stiener and Taborek [47] correlation now under-predicts the experimental results and gives heat transfer coefficient values that increase with increasing vapour quality like the behaviour of Liu and Winterton [32] correlation. This reflects the sensitivity of this correlation to tube diameter as will be discussed later. The performance of the other correlations for this tube data was similar to that in the 0.52 mm tube. The behaviour of all correlations did not change when the heated length increased to 300 and 450 mm for D = 1.1 mm (Fig.1(c) and (d)). Kandlikar [25] correlation predicts both the trend and magnitude of the heat transfer coefficient very well for the L = 450 mm tube and slightly under-predicts its magnitude in case of L = 300 mm.

Fig. 2(a) indicates that for the 0.52 mm tube all microscale correlations failed to capture the experimental trend except the correlations of Bertsch et al. [18] and Mahmoud and Karayiannis [31] that show similar trend if the first data point in the low quality region was excluded. Kew and Cornwell [22], Saitoh et al. [17] and Mikielewicz [24] correlations give a heat transfer coefficient that increases almost linearly with vapour quality. Warrier et al. [4] correlation predicts heat transfer coefficients that are much lower than the experimental values and remain almost constant with quality. Kandlikar and Balasubramanian [23] correlation predicts heat transfer coefficients that slightly decrease with quality up to a certain quality value after which the coefficient remains approximately constant with a further decrease at the high quality values. Zhang et al. [16] correlation behaves in a similar way to Chen [15] correlation where the coefficient increases with quality in the very low quality region with the effect of quality diminishing in the high quality region. The heat transfer coefficient predicted by the correlation of Lee and Mudawar [29] shows an N-shape trend, i.e. it increases with quality to a peak value at $x \approx 0.1$, then it decreases rapidly with quality up to $x \approx 0.55$ after which it jumps again to another peak value. Li and Wu [30] correlation predicts heat transfer coefficient values that show little dependence on vapour quality in the very small quality region and rapid decrease with vapour quality in the high quality region. It can be concluded from Fig. 2(a) that, there is an acceptable or approximate agreement between the experimental values and all microscale correlations over the qual-

Table A2
Existing macroscale correlations.

Reference	Correlation	Applicability range
Chen [15]	$h_{tp} = Sh_{F-Z} + Fh_L$ $h_L = 0.023\mathrm{Re}_L^{0.8}\mathrm{Pr}_L^{0.4}\frac{k_L}{D}$, $\mathrm{Re}_L = \frac{(1-x)GD}{\mu_L}$ $h_{F-Z} = 0.00122\frac{k_L^{0.79}c_{pL}^{0.45}\rho_L^{0.49}}{\sigma^{0.5}\mu_L^{0.29}h_{fg}^{0.24}\rho_v^{0.24}}(\Delta T)^{0.24}(\Delta P)^{0.75}$ $F = \begin{cases} 1 & 1/X_{tt} \leqslant 0.1 \\ 2.35(0.213 + \frac{1}{X_{tt}})^{0.736} & 1/X_{tt} > 0.1 \end{cases}$ $X_{tt} = \left(\frac{1-x}{x}\right)^{0.9}\left(\frac{\rho_v}{\rho_L}\right)^{0.5}\left(\frac{\mu_L}{\mu_v}\right)^{0.1}$ $S = \frac{1}{1+0.00000253\mathrm{Re}_{tp}^{1.17}}$ $\mathrm{Re}_{tp} = \mathrm{Re}_L.F^{1.25}$	–Water, methanol, cyclohexane, pentane, heptane, benzene (594 data points) –Vertical upward and downward flow in tubes and annuli –Pressure range of 1–34.8 bar –Liquid inlet velocity range of 0.06–4.5 m/s –Vapour quality range of 0.01–0.71 –Heat flux range of 6.2–2400 kW/m^2
Shah [45]	$h_{tp} = MAX(h_{cb}, h_{nb})$ $N_{Co} = \left(\frac{1-x}{x}\right)^{0.8}\left(\frac{\rho_g}{\rho_L}\right)^{0.5}$, $Bo = \frac{q}{Gh_{fg}}$ $h_L = 0.023\mathrm{Re}_L^{0.8}\mathrm{Pr}_L^{0.4}\frac{k_L}{D}$, $\frac{h_{cb}}{h_L} = \frac{1.8}{N_{Co}^{0.8}}$ For $N_{Co} > 1$: $\frac{h_{nb}}{h_L} = \begin{cases} 230Bo^{0.5} & Bo > 0.0003 \\ 1 + 46Bo^{0.5} & Bo < 0.0003 \end{cases}$ For $0.1 < N_{Co} < 1$: $\frac{h_{nb}}{h_L} = FBo^{0.5}\exp(2.74N_{Co} - 0.1)$ $F = \begin{cases} 14.7 & Bo > 0.0011 \\ 15.43 & Bo < 0.0011 \end{cases}$ For $N_{Co} < 0.1$: $\frac{h_{nb}}{h_L} = FBo^{0.5}\exp(2.74N_{Co} - 0.15)$	Valid over reduced pressure range of 0.004–0.8 Based on 780 data points
Gungor and Winterton [46]	$h_{tp} = Fh_L + Sh_{nb}$ $h_L = 0.023\mathrm{Re}_L^{0.8}\mathrm{Pr}_L^{0.4}\frac{k_L}{D}$ $h_{nb} = 55P_r^{0.12-0.434\ln R_p}(-\log P_r)^{-0.55}M^{-0.5}q^{0.67}$ $F = 1 + 24000Bo^{1.16} + 37(1/X_{tt})^{0.86}$ $S = \frac{1}{1+1.15\times10^{-6}F^2\mathrm{Re}_L^{1.17}}$	Water, R11, R12, R22, R113, R114, ethylene glycol Based on 4800 data points D = 2.95–32 mm P = 0.08–202.6 bar
Kandlikar [25]	$h_{tp} = MAX(h_{conv}, h_{nb})$ $h_{conv} = [1.136N_{Co}^{-0.9}(25Fr_{Lo})^c + 667.2Bo^{0.7}F_{fl}]h_{Lo}$ $N_{Co} = \left(\frac{1-x}{x}\right)^{0.8}\left(\frac{\rho_v}{\rho_{Lo}}\right)^{0.5}$, $h_{Lo} = 0.023\mathrm{Re}_{Lo}^{0.8}\mathrm{Pr}_L^{0.4}\frac{k_L}{D}$ $h_{nb} = [0.6683N_{Co}^{-0.2}(25Fr_{Lo})^c + 1058Bo^{0.7}F_{fl}]h_{Lo}$ c = 0 for vertical tubes	Water, R11, R12, R22, R113, R114, R152a, nitrogen and neon. Based on 5246 data points. D = 4.6–32 mm G = 13–8179 kg/m^2 s x = 0.001–0.987 P = 0.4–64.2 bar N_{Co} = 0.004–52.1
Liu and Winterton [32]	$h_{tp} = \sqrt{(Fh_{Lo})^2 + (Sh_{nb})^2}$ $h_{Lo} = 0.023\mathrm{Re}_{Lo}^{0.8}\mathrm{Pr}_L^{0.4}\frac{k_L}{D}$, $\mathrm{Re}_{Lo} = \frac{GD}{\mu_L}$ $h_{nb} = 55P_r^{0.12-0.434\ln R_p}(-\log P_r)^{-0.55}M^{-0.5}q^{0.67}$ $F = \left[1 + x\mathrm{Pr}_L\left(\frac{\rho_L}{\rho_g} - 1\right)\right]^{0.35}$, $S = \frac{1}{1+0.055F^{0.1}\mathrm{Re}_{Lo}^{0.16}}$	G = 12.4–8179.3 kg/m^2 s q = 348.9–2.62 × 10^6 W/m^2 x = 0–0.948 D = 2.95–32 mm Re = 568.9–8.75 × 10^5 P_r = 0.0023–0.895 Pr_L = 0.83–9.1
Stiener and Taborek [47]	$h_{tp} = [(h_{nb,0}F_{nb})^3 + (h_LF_{tp})^3]^{1/3}$ $h_{nb,0}$ = 3500 W/m^2 K for R134a $F_{nb} = F_{pf}\left(\frac{q}{q_0}\right)^{nf}\left(\frac{D}{D_0}\right)^{-0.4}\left(\frac{R_p}{R_{p,0}}\right)^{0.133}f(M)$ q_0 = 20,000 W/m^2 for R134a, D_0 = 0.01 m $R_{P,0}$ = 1 µm, R_P is surface roughness $F_{pf} = 2.816P_r^{0.45} + \left(3.4 + \frac{1.7}{1-P_r^7}\right)P_r^{3.7}$ nf = 0.8 - 0.1 exp (1.75P_r) $f(M)$ = 0.377 + 0.199 ln M + 0.000028427M^2 M = 102 for R134a $q_{ONB} = \frac{2\sigma T_{sat}h_L}{r_c\rho_g h_{fg}}$, r_c = 0.3 µm, $h_L = Nu_{Geniel}\frac{k_L}{D}$ For $q > q_{ONB}$ and $x \leqslant 0.6$: $F_{tp} = \left[(1-x)^{1.5} + 1.9x^{0.6}\left(\frac{\rho_L}{\rho_g}\right)^{0.35}\right]^{1.1}$ For $q < q_{ONB}$ and all values of x: $F_{tp} = \left\{ \left[(1-x)^{1.5} + 1.9x^{0.6}(1-x)^{0.01}\left(\frac{\rho_L}{\rho_g}\right)^{0.35}\right]^{-2.2} + \left[\frac{h_g}{h_L}x^{0.01}(1+8(1-x)^{0.7})\left(\frac{\rho_L}{\rho_g}\right)^{0.67}\right]^{-2} \right\}^{-0.5}$	Based on 10262 data points for water and 2345 data points for four refrigerants (R11, R12, R22, R113), seven hydrocarbons (benzene, n-pentane, n-heptane, cyclohexane, methanol, ethanol, n-butanol) and three cryogenics (nitrogen, hydrogen and helium)

ity range from 0.1 to 0.3, except for the correlations of Warrier et al. [4], Kandlikar and Balasubramanian [23] and Zhang et al. [16].

Fig. 2b indicates that for the 1.1 mm tube (L = 150 mm) only the correlations of Kew and Cornwell [22] and Mikielewicz [24] agree with the experimental trend and values very well. The correlations of Saitoh et al. [17], Bertsch et al. [18] and Li and Wu [30] agree very well with the experimental values only in the low quality region (up to $x \approx 0.3$). The correlation of Mah-

Table 1
The vapour quality range at which dryout occurred for each test section.

Diameter/length, mm	0.52/100	1.1/150	1.1/300	1.1/450
Dry out quality range				
G > 200 kg/m^2	Same for entire mass	Up to $x \approx 0.55$	Up to $x \approx 0.65$	Up to $x \approx 0.85$
G < 200 kg/m^2	Flux range – no dryout up to $x \approx 0.9$	Up to $x \approx 0.85$	Up to $x \approx 0.88$	Up to $x \approx 0.90$

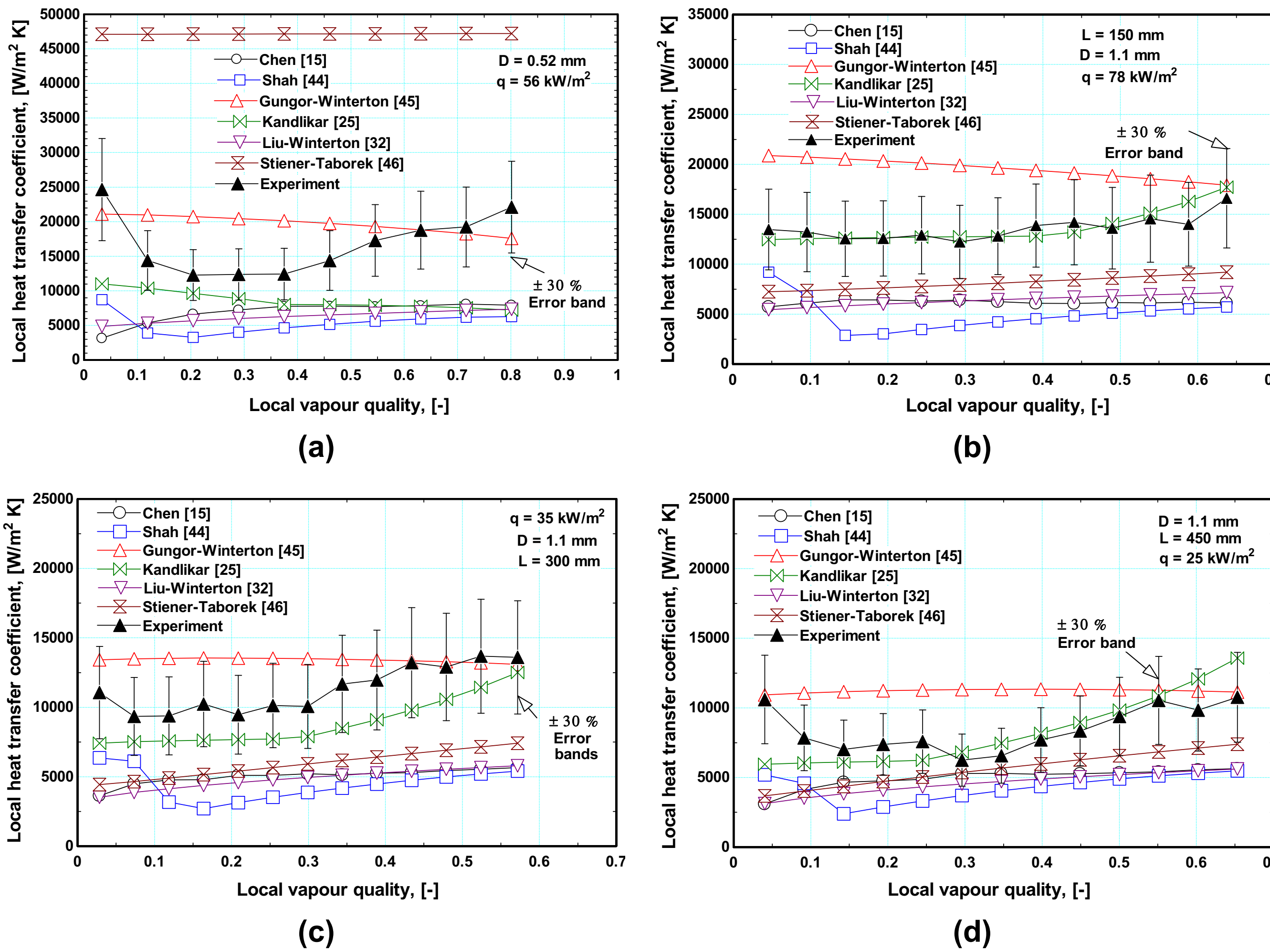

Fig. 1. The local comparison with the examined macroscale correlations at $G = 300$ kg/m^2 s, $P = 6$ bar and a selected value of heat flux; (a) $D = 0.52$ mm, $L = 100$ mm, (b) D = 1.1 mm, $L = 150$ mm, (c) D = 1.1 mm, $L = 300$ mm, (d) D = 1.1 mm, $L = 450$ mm.

moud and Karayiannis [31] predicts higher values in the low quality region but gets progressively better with quality. All other correlations deviate significantly from the experimental values. Fig. 2(c) indicates for the 1.1 mm tube with $L = 300$ mm that all correlations disagree with the experimental values except the correlation of Li and Wu [30] and Mahmoud and Karayiannis [31], which agreed very well but only up to $x \approx 0.3$. At higher quality values the predictions are still within the error band. In Fig. 2(d) for $L = 450$ mm, only the correlations of Mikielewicz [24], Bertsch et al. [18] and Saitoh et al. [17] agreed well with the data but again only over the quality range 0.1–0.4. The correlations of Li and Wu [30] and Mahmoud and Karayiannis [31] exhibited similar behaviour and predicted reasonably the values over all quality values. It is worth noting that none of the examined microscale correlations could predict the experimental trend very well. They could not predict the increasing trend of the heat transfer coefficient observed at high quality values. It is obvious that the performance of some correlations varies with the variation of the heated length.

4.2. Global assessment

4.2.1. Macroscale correlations

Table 2 summarizes the statistical assessment of the six examined macroscale correlations while Fig. 3 illustrates the global comparison with these correlations. It is clear that Kandlikar [25] and Gungor and Winterton [46] correlations perform much better than the rest. A more detailed discussion on the performance of the correlations is given below.

4.2.1.1. Kandlikar correlation. Kandlikar [25] correlation predicted 55.5% of all data within the ±30% error band at a MAE value of 75.9%. For the 0.52 mm tube, it under-predicts the data with β/MAE values of 45.2/40.1% respectively. For the shortest 1.1 mm

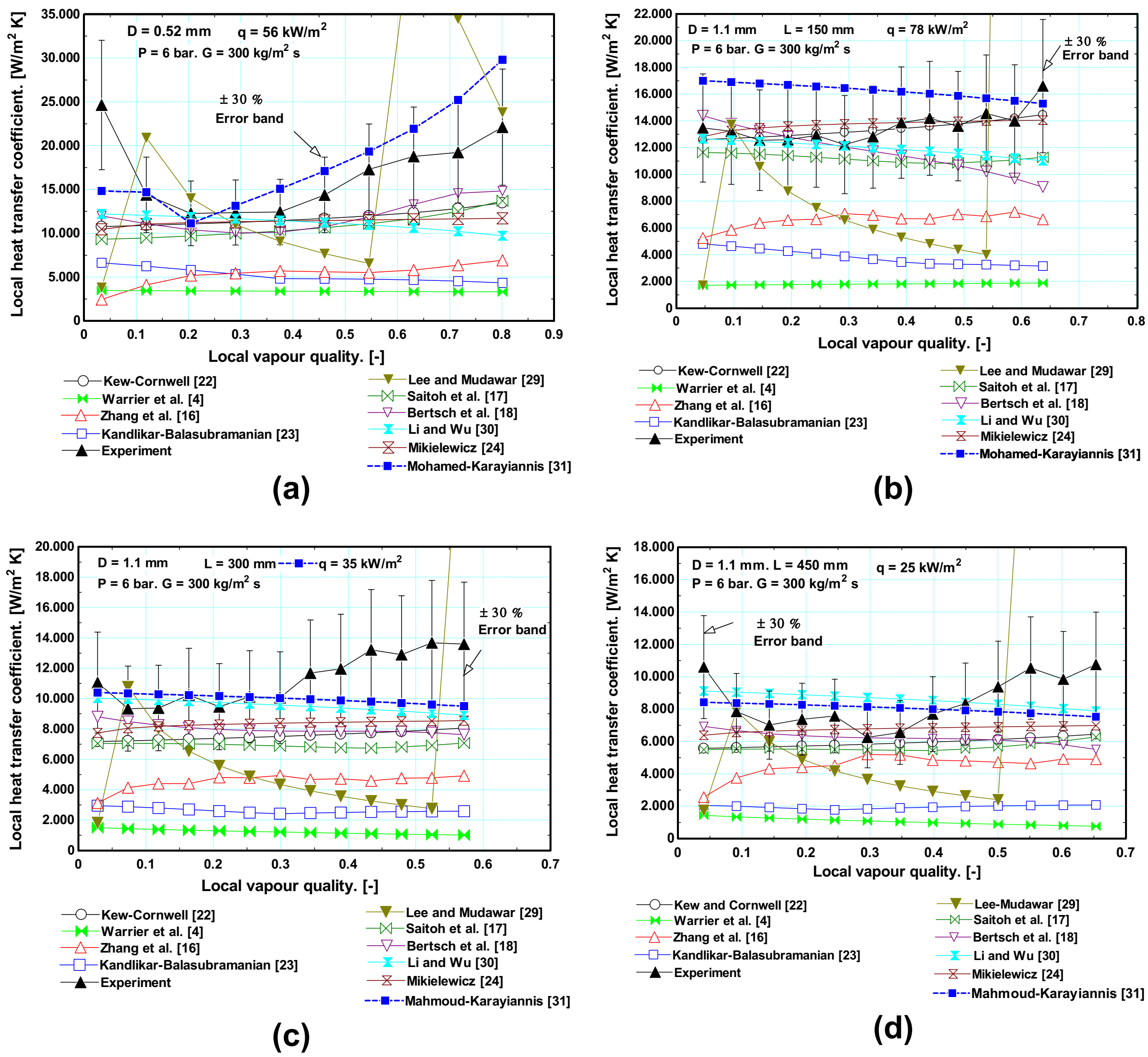

Fig. 2. The local comparison with the examined microscale correlations at $G = 300\ kg/m^2\ s$, $P = 6$ bar and a selected value of heat flux; (a) $D = 0.52$ mm, $L = 100$ mm, (b) $D = 1.1$ mm, $L = 150$ mm, (c) $D = 1.1$ mm, $L = 300$ mm, (d) $D = 1.1$ mm, $L = 450$ mm.

Table 2
The statistical assessment of the six examined macroscale correlations.

Correlation	Diameter/length, mm								All data	
	0.52/100 mm		1.1/150 mm		1.1/300 mm		1.1/450 mm			
	β	MAE	β	MAE	β	MAE	β	MAE	β	MAE
Chen [15]	27.2	69.8	0.2	66.1	10.6	106.2	21	70.7	14	92.3
Shah [45]	11.8	60.1	15	56.8	12.5	47.3	10.4	60.4	12.7	58.3
Gungor-Winterton [46]	36.7	62.8	50.2	33.4	47.2	58.7	47	66.5	45.7	55.4
Kandlikar [25]	45.2	40.1	68	32.3	45.5	49.6	45.5	50.3	55.5	75.9
Liu and Winterton [32]	18.7	54.4	0.3	60.3	0.4	60.6	15.6	60.6	8.9	59.3
Steiner-Taborek [47]	1.1	237	4.3	48.4	15.8	52.8	27	54.4	12.7	91.3

dia. tube ($L = 150$ mm), the correlation gives very good predictions compared to the other correlations with β/ MAE values of 68/32.3%. On the other hand, for the tube with $L = 300$ and 450 mm, the performance of the correlation was the same with a MAE value of about 50% and about 45% of the data within the ±30% error bands. Fig. 1 explains the performance of the Kandlikar [25] correlation in the global comparison. Fig. 1(a) indicates that for the 0.52 mm dia. tube there is some agreement between the predicted and experimental values over a narrow range of vapour quality ($x \approx 0.1$–0.3) with magnitudes less than the experiment. This is clear from Fig. 3(a) where the correlation under-predicts most of the data in this tube. On the contrary, the correlation captured the correct experimental trend and magnitudes in the shortest 1.1 mm dia. tube up to $x = 0.7$. The over-prediction depicted in Fig. 3 for the $D = 1.1$ mm tube was found to occur at vapour qualities greater than 0.7. According to the correlation (see Table A2), as the quality approaches unity the convection number (Nco) approaches zero and thus the heat transfer coefficient approaches infinity. This creates a very high over-estimation for the heat transfer coefficient at very high vapour quality values. So, it can be concluded that Kan-

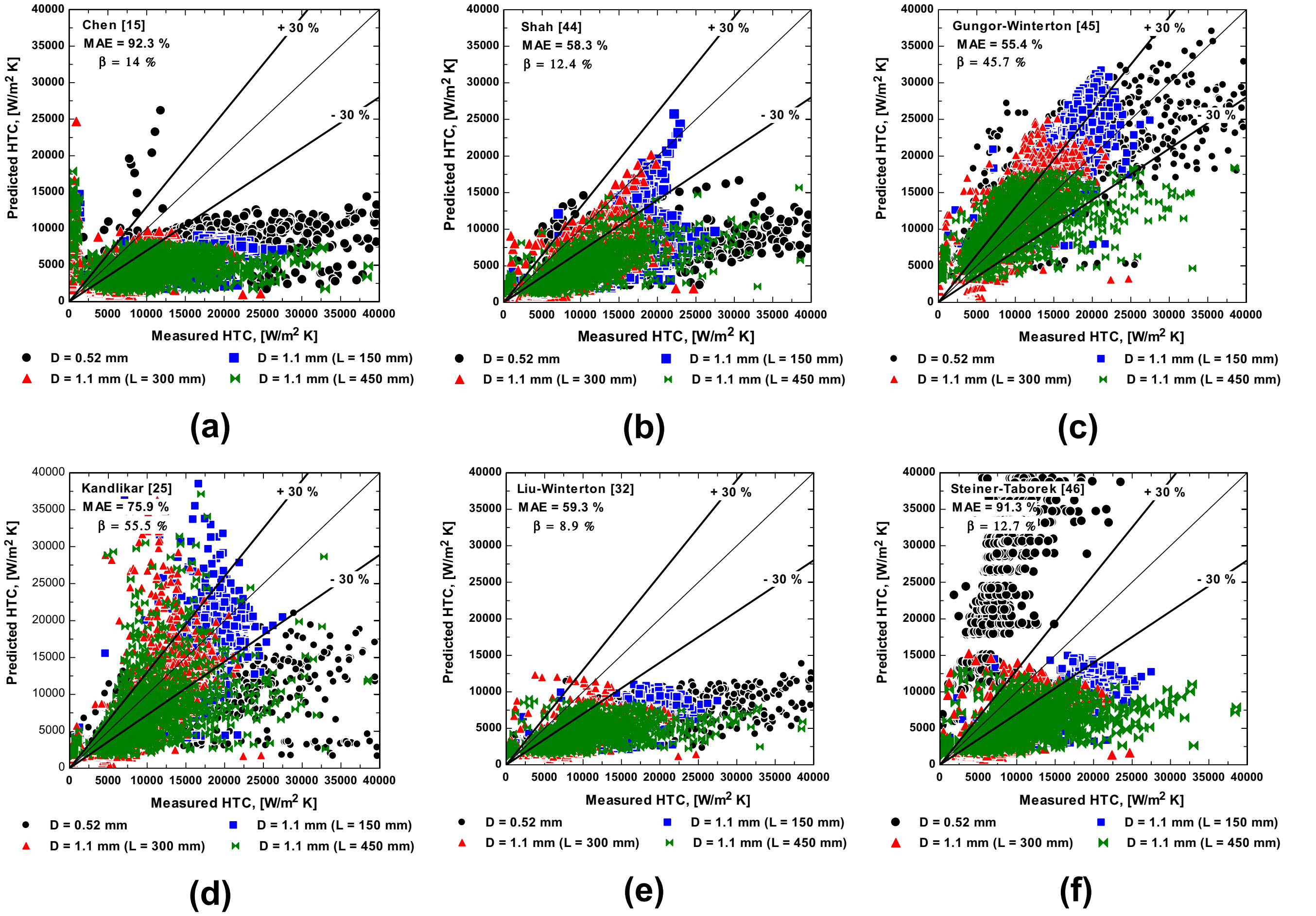

Fig. 3. The global comparison with the six macroscale correlations; (a) Chen [15], (b) Shah [45], (c) Gungor and Winterton [46], (d) Kandlikar [25], (e) Liu and Winterton [32], (f) Steiner and Taborek [47].

dlikar [25] correlation tends to under-predict the experimental values up to intermediate vapour quality values and over-predicts the values at high vapour qualities.

4.2.1.2. Gungor and Winterton correlation. Gungor and Winterton [46] correlation predicted 45.7% of all data within the ±30% error band at a MAE value of 55.4%. Table 2 indicates that the correlation predicts 36.7% of the micro-tube data within the ±30% error bands with a MAE value of 62.8%. On the other hand, the prediction gets better in the 1.1 mm diameter tubes particularly in the tube with the shortest heated length, where the correlation predicted 50.2% of the data within the ±30% error bands with a MAE value of 33.4%. The performance of the correlation in all tubes can be explained using Fig. 1. The correlation gives a heat transfer coefficient that is almost independent of vapour quality in the low quality region and it decreases slightly with quality in the high quality region. This trend is consistent with the experimental trend in the tube with heated length of 150 mm. However, the correlation over-predicts the experimental values at high heat flux values. In other words, the correlation works reasonably at low to intermediate heat flux values. The over-estimation of the heat transfer coefficient at high heat fluxes could be attributed to the inclusion of the boiling number in the convective boiling enhancement factor (F). This means that, the heat flux effect was considered in the convective boiling term as well as the nucleate boiling term. The exponent of (q) was 0.67 in the nucleate boiling term and 1.16 in the convective boiling term. As a result, increasing the heat flux by small values will result in very high increments of the heat transfer coefficient that exceed the experimental values. As the heated length increased, the experimental heat transfer coefficient exhibited some dependence on vapour quality after $x = 0.3–0.4$ where the coefficient increased with vapour quality. This quality effect was not predicted by the correlation and this resulted in a higher mean absolute error compared to the 150 mm heated length.

4.2.1.3. Chen correlation. Chen [15] correlation predicted only 14% of all data within the error band at a MAE value of 92.3%. Fig. 1 indicates that the Chen correlation gives a heat transfer coefficient that moderately increases with increasing vapour quality in the very low quality region and then shows a plateau as the quality increases. The behaviour of the correlation at very low vapour quality values is opposite to the experimental behaviour where the heat transfer coefficient drops from its maximum value at $x \cong 0$. Accordingly, the maximum deviation between the predicted and measured values is expected to occur at very low vapour quality values and also at high vapour quality values when the experimental heat transfer coefficient exhibits an increasing trend with vapour quality. The global high deviation between the Chen correlation and the experimental values may be attributed to the fact that the correlation was developed using data for water and hydrocarbons only. These fluids have a much higher surface tension compared to R134a, which significantly influences the bubble departure diameter and the characteristics of the flow patterns. Another reason could be the accuracy of the nucleate pool boiling correlation of Forster and Zuber [20] which gives much lower values than the Cooper [21] correlation, the later taking into account the effect of fluid type, surface roughness, heat flux and reduced pressure.

4.2.1.4. Shah correlation. Shah [45] correlation predicted only 12.7% of all data within the error bands at a MAE value of 58.3%. As presented in Fig. 1, the heat transfer coefficient predicted by the Shah [45] correlation drops from a high value at very low vapour quality and then it increases constantly with increasing vapour quality. This trend was similar to the current experimental trend. Inspecting the performance of the correlation at different experimental conditions (not shown in the figure) demonstrated that the correlation tends to work better in the very low quality region, at high system pressure, and at very high vapour quality. This can be explained as follows: as system pressure increases, the latent heat decreases and consequently the boiling number increases. In their correlation (see Table A2), the nucleate boiling term was introduced as a function of the boiling number only. Therefore, increasing heat flux at high system pressure (increasing boiling number) results in high magnitudes of the predicted heat transfer coefficient in the very low quality region (nucleate boiling) which are close to the experimental values. Additionally, as the vapour quality increases to high values, the magnitude of the convection number becomes very small and consequently the convective heat transfer coefficient becomes too large. It approaches infinity as x approaches 1. Therefore, a small number of data points matched the experimental values at these conditions (high pressure, very low and very high quality). The global tendency of the correlation to under-predict significantly the experimental values could be due to the use of the boiling number only to correlate the nucleate boiling term. The boiling number includes only the latent heat as a fluid property. This means that other parameters such as surface roughness, fluid properties and reduced pressure that influence significantly the nucleate boiling heat transfer rates were not taken into consideration.

4.2.1.5. Liu and Winterton correlation. The Liu and Winterton [32] correlation predicted only 8.9% of all data within the error band at a MAE value of 59.3%. This correlation looks similar in performance to Chen [15] correlation though the method of combining the contribution of the nucleate and convective boiling is different. The differences between the Liu-Winterton correlation and the others are that the single phase liquid heat transfer coefficient and the nucleate boiling suppression factor were calculated based on the all-liquid Reynolds number rather than using the liquid Reynolds number, i.e. using G not $(1-x)G$.

4.2.1.6. Steiner and Taborek correlation. Steiner and Taborek [47] asymptotic model predicted only 12.7% of all data within the error band at a MAE value of 91.3%. Fig. 3(f) indicates that the correlation over-predicts significantly the experimental data of the 0.52 mm dia. tube, while it tends to under-predict most of the data of the 1.1 mm dia. tube. It is very clear from Eq. (4) that, the correlation takes into consideration the effect of tube diameter in the nucleate boiling factor (F_{nb}). The nucleate boiling factor increases and consequently the heat transfer coefficient increases as the diameter decreases. Increasing the diameter from 0.52 to 1.1 mm resulted in a decrease in the normalised diameter term in Eq. (4) by 26%.

$$F_{nb} = F_{pf}\left(\frac{q}{q_0}\right)^{nf}\left(\frac{D}{D_0}\right)^{-0.4}\left(\frac{R_p}{R_{p,0}}\right)^{0.133} f(M) \tag{4}$$

4.2.2. Microscale correlations

Table 3 summarizes the statistical assessment of the examined microscale correlations while Fig. 4 depicts the global comparison. It is worth mentioning that the Cooper pool boiling correlation is included here for the sake of comparison though it is not a microscale correlation. The performance of each correlation is assessed in more detail as given below.

4.2.2.1. Mahmoud and Karayiannis correlation. It is obvious from the table that all correlations failed to predict the experimental data reasonably well, except the correlation of Mahmoud and Karayiannis [31]. This correlation predicted 87.3% of the data within the ±30% error bands at a MAE value of 15.9%, see Fig. 4(m). Although Mahmoud and Karayiannis [31] excluded the data of the two longest 1.1 mm diameter tubes when developing the correlation, it could still predict the data of these longest tubes reasonably. The performance of this correlation is much better than all examined correlations, see Table 3.

4.2.2.2. Zhang et al. correlation. The second best examined correlation was that of Zhang et al. [16] but modified by using the Cooper [21] correlation for the nucleate boiling term as proposed by Karayiannis et al. [48], instead of using Forster-Zuber [20] found in the original correlation, see Fig. 4g. It predicted 68.4% of all data within the ±30% error bands with a MAE value of 41%. It is worth mentioning that the original Zhang et al. [16] correlation predicted only 12.6% of all data within the error bands with a MAE value of 103% as shown in Fig. 4(f). Although the original Zhang et al. [16] correlation is a modified version of the Chen [15] correlation, it is clear that the correlation does not add any improvements in predictability. Fig. 2 indicates that, the behaviour of the predicted local heat transfer coefficient using Zhang et al. [16] original correlation is similar to that predicted by Chen [15] correlation. Both correlations predict a heat transfer coefficient that increases rapidly with quality in the very low quality region and increases very slowly with quality in the high quality region, which is different from the experimental trend.

4.2.2.3. Cooper pool boiling correlation. Cooper [21] correlation was next in global performance, see Fig. 5. It predicted 63.7% of all data within the ±30% error bands with a MAE value of 35% which is much better than the assessed macro and microscale correlations. The performance of the Cooper correlation for each tube is indicated in Table 3. It predicted 51.5% of the micro tube data within the ±30% error bands and 85% of the shortest mini tube data within the ±30% error bands. As the heated length increased, the performance of the correlation deteriorates compared to the shortest tube. The performance of this correlation looks very consistent with the experimental results for each tube. In the 0.52 mm dia. tube, nucleate boiling appears to dominate up to a vapour quality value of about 0.4 (mid quality range). This means that about 50% of the data in this tube (data with $x < 0.4$) may be in the nucleate boiling regime, which agrees with the correlation where 51.5% of the data were predicted very well. By contrast, the experiment indicated that all data before dryout (see Table 1) of the shortest 1.1 mm dia. tube ($L = 150$ mm) could be in the nucleate boiling regime. Therefore the correlation performed very well with this tube. As the heated length of the 1.1 mm dia. tube was increased, both nucleate and convective boiling exists, which makes the performance of the correlation worse.

4.2.2.4. Li and Wu correlation. The correlations of Li and Wu [30] and Mikielewicz [24] follow the order of ability to predict the experimental data. Li and Wu [30] correlation predicts heat transfer coefficient values that decrease very slowly and at a higher rate in the low and high quality region respectively, see Fig. 2. The cor-

Table 3
The statistical assessment of the examined microscale correlations including Cooper [21] pool boiling correlation.

Correlation	Diameter/length, mm								All data	
	0.52/100 mm		1.1/150 mm		1.1/300 mm		1.1/450 mm			
	β	MAE	β	MAE	β	MAE	β	MAE	β	MAE
Lazarek-Black [27]	43.7	51.6	65.8	32.2	38.4	42	23.8	45.2	42.4	43.5
Trant et al. [28]	2.4	69.3	3.5	50.7	3.1	54.6	2.7	56.8	2.9	58.7
Kew-Cornwell [22]	52.7	32.5	69.1	25.7	49.7	44.2	34.2	53.2	52.5	39.8
Warrier et al. [4]	7	76.8	1.8	77.4	0.4	88	0.6	84.7	1.8	85.6
Kandlikar-Balasubramanian [23]	2	68.9	7.8	62.3	2	65.2	1.8	69	2.3	66.4
Zhang et al. [16]	11.4	79.7	1.5	64.2	15	122.6	21	133.6	12.6	103
Zhang et al. [16][a]	66.1	33.7	77	24.8	72.6	46.2	57	55.6	68.4	41
Lee-Mudawar [29]	31.4	73.9	19.5	119.5	20.3	133.3	18	132.7	21.9	117.5
Saitoh et al. [17]	45.3	39.1	73.9	27.7	63.3	46.7	54	56.8	59.6	43.3
Bertsch et al. [18]	54.7	37.6	58.8	28.8	62.8	39.1	45.1	50.1	57	38.8
Mikielewicz [24]	49.5	34.8	76.3	21.8	65.3	38.4	45.8	49.1	60	36.5
Li-Wu [30]	43	58.4	69.8	26.2	70	64.4	52.3	70.6	60.1	56
Cooper [21]	51.5	34.4	85	19.3	69.3	36.2	47.1	49	63.7	35
Mahmoud and Karayiannis [31]	86.8	16.5	91.7	14.6	87.4	15.1	83.3	17.6	87.3	15.9

[a] Modified using Cooper pool boiling correlation.

relation predicts 60.1% of all data within the error bands at a MAE value of 56%. Table 3 indicates that for the 0.52 mm dia. tube, the correlation predicts only 43% of the data within the error bands with a high MAE value of 58.4%. The performance of the correlation improves in the 1.1 mm dia. tube with heated lengths of 150 and 300 mm where about 70% of the data were predicted within the error bands. However, the MAE value in the 1.1 mm dia. tube with L = 150 mm was less than 30% compared to 64.4% for L = 300 mm. The value of the MAE is usually influenced by the heat transfer coefficient value at the first location in the very low quality region and the delay in boiling incipience. As the heated length increased to 450 mm, the correlation predicted only 52.3% of the data within the error bands with MAE value of 70.6%. It can be concluded that, the correlation highly under-predicts the experimental values in the high quality region particularly when the measured heat transfer coefficient increases with vapour quality. The heat transfer coefficient predicted by this correlation depends on heat and mass flux with exponents 0.3 and -0.156 respectively which reflects the small effect of these two parameters. The correlation predicts that the heat transfer coefficient increases with decreasing tube diameter with an exponent of D being 0.456. Some investigators such as Saitoh et al. [17], Karayiannis et al. [48] and Consolini and Thome [49] reported that the heat transfer coefficient increases with decreasing tube diameter.

4.2.2.5. Mikielewicz correlation. Mikielewicz [24] correlation could predict up to 60% of all data within the error bands. Its performance is significantly influenced by the variation of the heated length of the 1.1 mm diam. tube. For the shortest tube, the correlation predicted reasonably 76.3% of the data with a MAE value of 21.8%. For L = 300 mm it predicted only 65.3% of the data within the error bands and this value decreased to 45.8% when the heated length increased to 450 mm. Fig. 2 illustrates that the correlation predicts heat transfer coefficient values that increase moderately with increasing vapour quality. This may explain the success of the correlation in predicting the data of the shortest tube where the heat transfer coefficient was independent of vapour quality.

4.2.2.6. Bertsch et al. correlation. The correlations of Bertsch et al. [18], Saitoh et al. [17] and Kew and Cornwell [22] demonstrated approximately similar performance. The global comparison of the present data with the correlation of Bertsch et al. is depicted in Fig. 4(j). It predicts only 57% of all data within the error bands at a MAE value of 38.8%. The correlation predicted about 55% of the 0.52 mm dia. tube data within the error bands with an error value of 37.6%. For the 1.1 mm dia. tube with L = 150 and 300 mm, the performance of the correlation was almost similar, with about 60% of the data predicted within the error bands. As the heated length increased to 450 mm, the prediction gets worse and only 45.1% of the data were predicted within the error bands. Looking at Fig. 2(a) for the 0.52 mm dia. tube, the correlation predicted heat transfer coefficient values that increase with vapour quality towards the exit, which is similar to the experimental trend. For the 1.1 mm dia. tube, the correlation predicted heat transfer coefficient that sharply (Fig. 2(b)) or slightly decreases with vapour quality (Fig. 2(c) and (d)). This behaviour may be attributed to the functional form selected for the nucleate boiling suppression factor and the convective boiling enhancement factor. The convective boiling enhancement factor was correlated using the confinement number but gives values that contradict the confinement principle. Confinement effects are significant when the confinement number is in excess of 0.5. So, it is expected that the higher the confinement number, the higher the enhancement in convective boiling. However, the proposed correlation for the convective boiling gives values that increase with decreasing the confinement number. Also, for a fixed value of the confinement number, the enhancement factor reaches a peak value at $x \approx 0.78$ after which it rapidly decreases with increasing vapour quality. Additionally, introducing the nucleate boiling suppression factor as a function of vapour quality only may not be enough. Nucleate boiling suppression seems to be influenced strongly by other parameters, such as flow velocity and fluid properties that affect strongly the characteristics of the boundary layer next to the wall. The rapid decrease in the heat transfer coefficient with increasing vapour quality that was observed only in the shortest 1.1 mm dia. tube (L = 150 mm) can be attributed to the operation at much higher heat flux values compared to the other tubes. This results in much higher nucleate pool boiling heat transfer coefficient according to Cooper [21] correlation, which when it is multiplied by the suppression factor $(1-x)$, results in the rapid decrease with quality.

4.2.2.7. Saitoh et al. correlation. Saitoh et al. [17] correlation predicted only 55.6% of the data within the error bands at a MAE value of 43.3% as seen in Fig. 4i. According to Fig. 2 the correlation predicts that the heat transfer coefficient increases moderately with quality in the 0.52 mm dia. tube while it decreases very slightly with vapour quality in the 1.1 mm tubes. In all tubes, the coefficient jumps to a very high value as the quality approaches to 1 (not shown in Fig. 2). Also, by inspecting the performance of the correlation at different operating conditions (not shown in Fig. 4), it was found that the correlation highly under-predicts the data at low heat flux values. Similar to the abovementioned

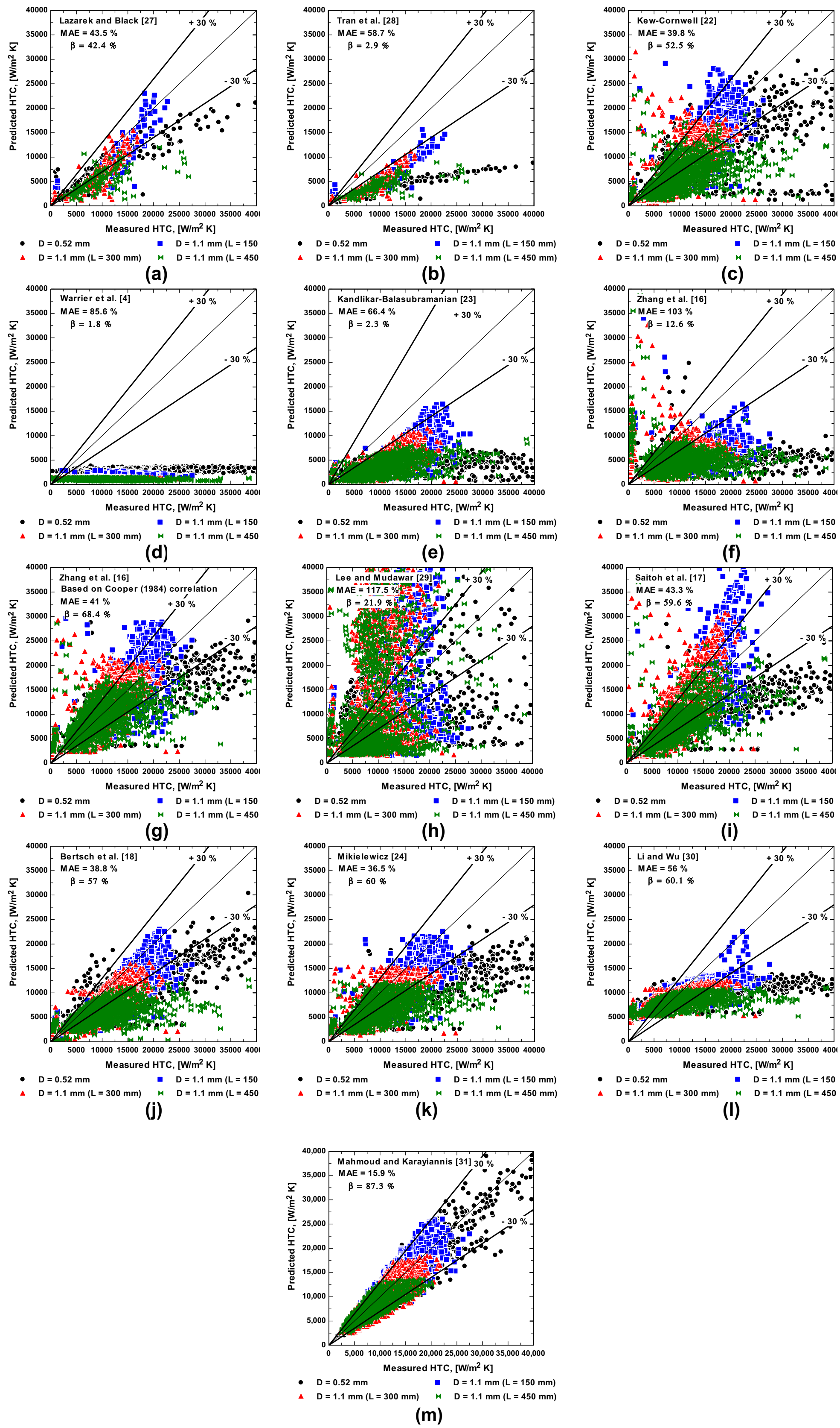

Fig. 4. The global comparison with the examined microscale correlations; (a) Lazarek and Black [27], (b) Tran et al. [28], (c) Kew and Cornwell [22], (d) Warrier et al. [4], (e) Kandlikar and Balasubramanian [23], (f) Zhang et al. [16], (g) modified Zhang et al. [16], see [48] (h) Lee and Mudawar [29], (i) Saitoh et al. [17], (j) Bertsch et al. [18], (k) Mikielewicz [24], (l) Li and Wu [30], (m) Mahmoud and Karayiannis [31].

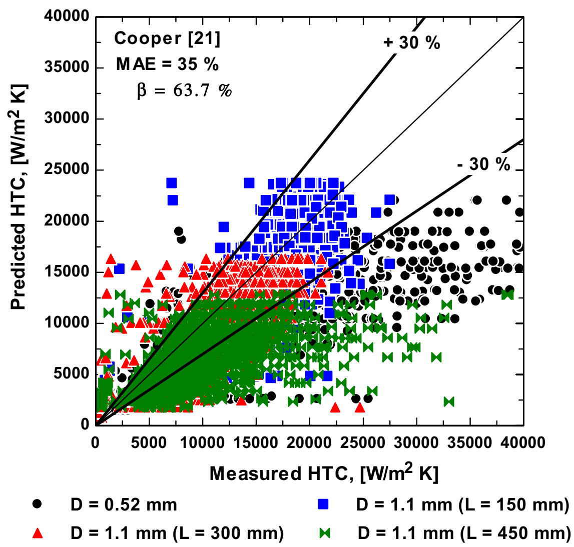

Fig. 5. Global comparison with Cooper [21] pool boiling correlation.

correlations, the performance of this correlation gets worse as the heated length increases. Although this correlation was developed for R134a and tubes with diameter ranging from 0.51 to 10.92 mm, it failed to predict reasonably the data of the current study (R134a). This may be attributed to the following reasons: (i) the heated length of the examined tubes in their study was too long compared to the one used in the present study, i.e. 500 mm versus 100 mm for $D = 0.5$ mm and 935 mm versus 150, 300, 450 mm for $D = 1.1$ mm. The heated length influences the operating heat flux value, i.e. for the same exit quality a high heat flux value is required in short tubes compared to long ones. The long heated length as well as the low operating heat flux values may influence the magnitude and trend of *h vs. x*. (ii) the experimental procedures in their study was different compared to that followed in the present study. In their experiment, they avoided the boiling incipience-related issues through triggering boiling using a valve located ahead of the test section while in the present study boiling was triggered normally inside the test section. Boiling incipience might influence the history of the heat transfer process. (iii) They conducted their experiments in horizontal tubes compared to vertical tubes used in the present study, i.e. possible stratification effects.

4.2.2.8. Kew and Cornwell correlation. Kew and Cornwell [22] correlation predicted only 52.5% of the data within the error bands at a MAE value of 39.8% as seen in Fig. 4(c). Since the correlation is a modified version of Lazarek and Black [27] correlation, the difference in performance is not that large (see Fig. 4(a) for the comparison with [27]). The performance of Kew and Cornwell [22] correlation can be explained using Fig. 2. The correlation predicts that the heat transfer coefficient increases at a slow rate with quality in the very low quality region and at a relatively faster rate in the high quality region. However, the slope of the *h–x* curve predicted by the correlation is much smaller than the slope of the experimental curve particularly after $x \approx 0.3–0.4$ for all tubes. Accordingly, the correlation deviates significantly from the experimental values at $x > 0.4$ and at the first data point for all tubes except the shortest 1.1 mm dia. tube. In this tube, the experimental slope of the *h–x* curve was very small, i.e. the coefficient was independent of vapour quality, which is close to the predicted slope by the correlation. This may explain why the correlation succeeded to predict 69.1% of the data in this tube with a small error value of 25.7%.

4.2.2.9. Lazarek and Black correlation. Lazarek and Black [27] correlation predicted 42.4% of the data within the error band at a MAE value of 43.5%. It predicted only 43.7% of the data of the 0.52 mm dia. tube within the error bands with a mean absolute error value of 51.6%. Its performance is consistent with the behaviour of the measured heat transfer coefficient in this tube. The measured coefficient drops from maximum value at $x \approx 0$, then it remains approximately constant over $x \approx 0.1–0.4$. Following that it increases continuously with quality. Since the correlation predicts that the heat transfer coefficient remains constant with quality, it is expected that the correlation highly under-predicts the experimental values at $x < 0.1$ and $x > 0.4$. On the other hand, the correlation performed much better in the shortest 1.1 mm dia. tube with MAE of 32.15% and 65.8% of the data within the error bands whilst the prediction gets worse as the heated length increases. Its success in predicting most of the data in the shortest tube is attributed to the dominance of nucleate boiling over all quality values. As the heated length of the 1.1 mm dia. tube increases, nucleate boiling prevailed in the low to intermediate quality region and convective boiling prevailed in the high quality region. The correlation was developed based on the fact that nucleate boiling is the only dominant mechanism and thus the predictions deteriorate as the heated length increases due to contribution of nucleate and convective boiling.

4.2.2.10. Tran et al. correlation. The correlations of Tran et al. [28], Warrier et al. [4] and Kandlikar and Balasubramanian [23] predicted very poorly the experimental data, see Fig. 4(b), (d) and (e). Tran et al. [28] correlation predicted only 2.9% of the data within the error band. The correlations of Tran et al. [28] and Lazarek and Black [27] and the experimental results of the shortest 1.1 mm dia. tube ($L = 150$ mm) agree on the dominance of nucleate boiling mechanism. However, there is a big difference in the performance of these two correlations compared to the actual experimental data of this tube. The study of Tran et al. and Lazarek and Black were conducted using the same fluid and almost similar tube diameter and thus the difference in performance may be attributed to the following reasons: (i) difference in tube material. Tran et al. and Lazarek and Black investigated a brass tube and a stainless steel tube respectively. Brass is more ductile than stainless steel and therefore the inner surface characteristics and consequently nucleation characteristics and heat transfer coefficient can be different. This effect can be deduced from the exponent of the boiling number in the correlations, i.e. Tran et al. indicates that the heat flux effect is less compared to Lazarek and Black; (ii) difference in the investigated heated lengths, 124 mm in [27] and 870 mm in [28]. Karayiannis et al. [14] reported that increasing the heated length results in a reduction in the heat transfer coefficient for the same exit quality. This factor explains why the Tran et al. correlation highly under-predicts the experimental data; (iii) reported effect of tube diameter, i.e. in the Tran et al. correlation, a decrease in the tube diameter results in a decrease in the heat transfer coefficient, which is contrary to the trend in Lazarek and Black.

4.2.2.11. Warrier et al. correlation. Warrier et al. [4] correlation predicted 1.8% of the data within the error bands at a MAE value of 85.6%. The high deviation could be attributed to the following reasons: (i) Type of fluid. There is a big difference between the properties of R134a refrigerant and dielectric FC84, particularly surface tension, latent heat and molecular weight. Compared to R134a, the surface tension value of FC84 is about 150% higher, the latent heat is about 50% less and the molecular weight is 380% higher. These three properties play a significant role in nucleate pool boiling heat transfer. The smaller the surface tension, the smaller the bubble departure diameter and consequently the higher the heat transfer coefficient, see also Stephan and Abdelsalam [19]. Cooper [21] pool boiling correlation predicts that the heat transfer coefficient decreases for fluids with high molecular weight. Accordingly, the heat transfer coefficient of FC84 is expected to be much smaller than that of R134a possibly explaining the tendency of the correlation to highly under-predict the experimental values. (ii) Differences between the multi-microchannels arrangements compared to single tubes as well as the channel material. The multi-microchannels configuration could have uneven flow distribution to each channel and the prevalence of instabilities, which may influence the heat transfer characteristics.

4.2.2.12. Kandlikar and Balasubramanian correlation. Kandlikar and Balasubramanian [23] correlation predicted 2.3% of the data within the error band at a MAE value of 66.4%. Surprisingly, the performance of the correlation was very poor compared to the original Kandlikar [25] correlation, see Fig. 3(d), which calls for a comment. Kandlikar and Balasubramanian [23] presented the original version of the correlation with a small difference compared to [25], i.e. all equations were multiplied by the term $(1-x)^{0.8}$ which was not included in the original form. They did not comment on this term and it was unclear whether it was included as a new modification or not. At vapour quality values very close to zero, the magnitude of this term approaches unity and the effect on the predicted values is expected to be small. However, as the quality increases, the magnitude of this term becomes much smaller than unity and consequently the magnitude of the predicted heat transfer coefficient is expected to be much smaller than the values predicted by the original correlation.

4.2.2.13. Lee and Mudawar correlation. Lee and Mudawar [29] correlation predicted 21.5% of the data within the error bands at a MAE value of 117.5%, see Fig. 4(h). It predicts poorly the experimental values with a large scatter possibly due to the fact that it is not capable of predicting the correct experimental trend, see Fig. 2. The local heat transfer coefficient behaves according to an N-shape trend, which is completely different from the measured experimental trends in all tubes. So, the correlation has captured only a few number of experimental points and either under-predicted or over-predicted the others. The failure of this correlation to predict the current experimental data may be attributed to the fact that the correlation was developed for rectangular multi-microchannels using only a small number of data points for R134a. Another reason could be the difference in experimental methodology. The current experimental data were collected through increasing the heat flux gradually at constant pressure and mass flux. In [29], the mass flux was varied while the pressure and the heat flux were kept constant.

5. Assessment of mechanistic models

This section presents the assessment of the two mechanistic models proposed by Thome et al. [35] and Consolini and Thome [41]. Fig. 6 depicts the local comparison between the measured heat transfer coefficient and the three-zone model of Thome et al. [35] on the h–x plane at $P = 6$ bar and $G = 300$ kg/m^2 s. Fig. 7 shows the global comparison. The transition line from the coalescence bubble regime to the annular flow regime as determined experimentally by the present authors is also shown in Fig. 6, because the model was developed for elongated bubbles (slug) flow. It is clear from the figure that the predicted heat transfer coefficient jumps to a peak value at $x \approx 0$ and then decreases continuously with increasing vapour quality. The behaviour of the model near $x \approx 0$ agrees with the experimental behaviour but under-predicts significantly the values at the first thermocouple location. This could be due to the high local pressure increase associated with bubble growth at the onset of boiling ($x \approx 0$) that was not taken into consideration by the model. In other words, the local pressure does not vary linearly in the very low quality region, i.e. the region around boiling incipience. Local pressure significantly influences the local saturation temperature and consequently the heat transfer coefficient. Accordingly, the value of wall superheat at boiling incipience will be smaller than that calculated based on the linear assumption, i.e. the heat transfer coefficient at the onset of boiling is higher. As seen in Fig. 6(a), the model could not predict the increasing trend of the heat transfer coefficient with vapour quality in the 0.52 mm dia. tube and there is an global partial agreement only over a narrow quality range. This is also clear from the global comparison in Fig. 7 where the model predicted only 42% of the smaller tube data within the ±30% error bands at a MAE value of 39.2%, see also Table 4. It is worth noting that, Fig. 6 indicates that the model tends to match or under-predicts slightly the experimental values at low to intermediate heat fluxes for all tubes. On the other hand, the model tends to over-predict significantly the data at high heat fluxes, which is clear in Fig. 6(b) for the shortest 1.1 mm dia. tube. However, the model predicted the trend very well in this tube. The higher values predicted at high heat flux may be due to the strong effect of heat flux on the pair frequency that is used in the model. The frequency was calculated using an empirical equation based on an optimization study. It is worth mentioning that, the pair frequency significantly affects the magnitude of the predicted heat transfer coefficient and it shifts the predicted values up or down. Shiferaw et al. [8] assessed the three-zone evaporation model using experimental data for R134a and tubes with diameters of 4.26 and 2.01 mm. They reported that the model predicted satisfactorily the data and they referred to the features of the model that require further modifications, i.e. bubble frequency and initial film thickness. They also stated that the local pressure fluctuations and nucleation before the location of the onset of the confined bubble should be considered. The model performed very well in this shortest 1.1 mm dia. tube where it predicted 76% of the data within the ±30% error bands at MAE value of 24%. As the heated length increased (Fig. 6(c) and (d)), the heat transfer coefficient exhibited an increasing trend towards the exit, similar to the 0.52 mm dia. tube, which the model cannot predict. However, the performance of the model in the tube with $L = 300$ mm was similar to that in the shortest tube. It predicted 75.8% of the data within the ±30% error bands but at higher MAE value of 35.7%. The performance of the model deteriorated in the longest tube, i.e. it predicted only 55% of the data within the ±30% error bands at a MAE value of 48%.

Figs. 8 and 9 depicts the comparison of the local and the global values with Consolini and Thome [41] model at $P = 6$ bar and $G = 300$ kg/m^2 s for the 0.52 mm dia. tube and the shortest 1.1 mm dia. tube. All data included in the comparison are located within the applicability range of the model, i.e. $x_c < x < x_a$. It is clear from Fig. 8 that the model predicted reasonably the trend and magnitudes for some heat fluxes but under-predicted significantly the data of the 1.1 mm dia. tube (Fig. 8(b)). Fig. 9 indicates that the model predicts poorly the experimental values in all tubes with relatively better performance in the 0.52 mm dia. tube. It is worth noting that, the three-zone model performs better in the comparison of the average values (global comparison) than this new model though both models assume thin film evaporation. The reason could be the size of the data bank that was used to correlate the empirical parameters in the two models. In the recent model, only data for tubes with diameters 0.51 and 0.79 mm and fluids R134a, R245fa and R236fa were used. In the 3-zone model, the empirical parameters were optimised using a larger data bank consisting of various fluids and tube diameters.

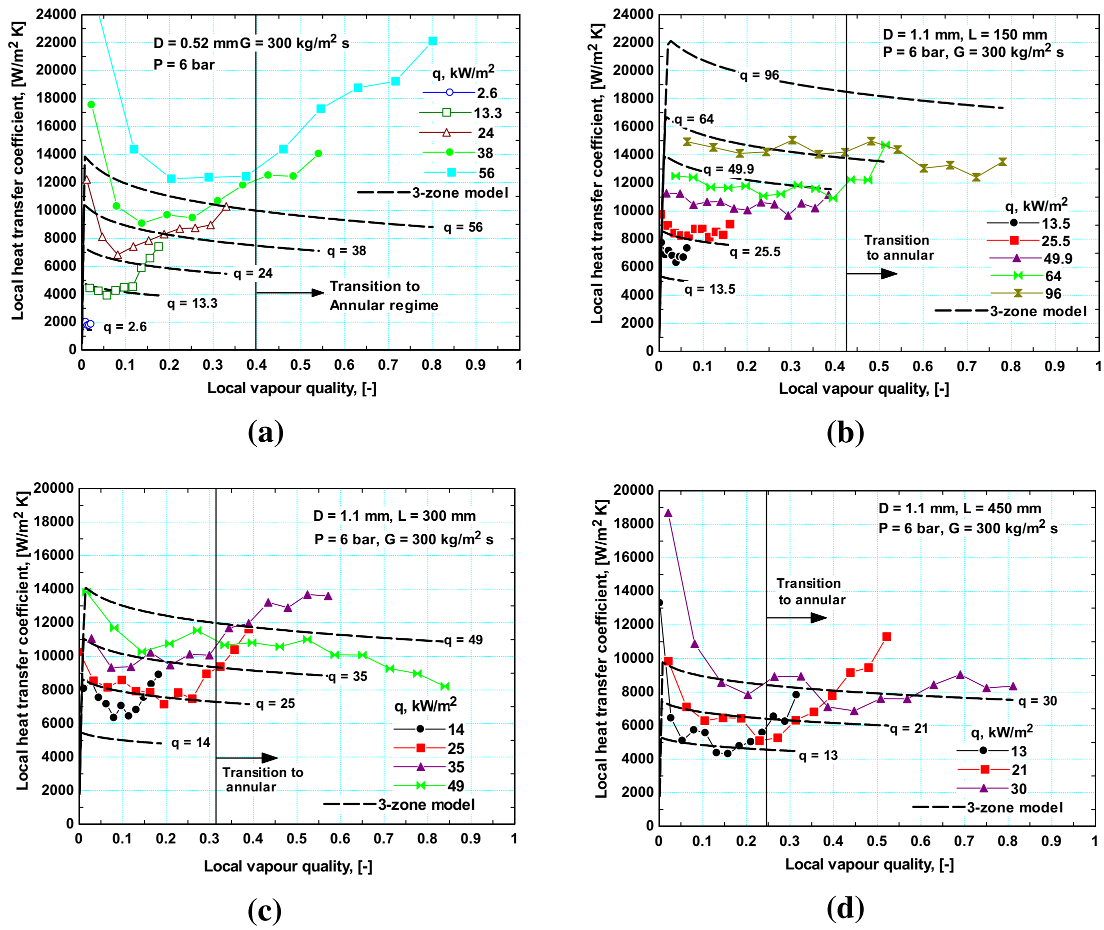

Fig. 6. Local comparison with Thome et al. [35] three zone model at $G = 300$ kg/m^2 s, $P = 6$ bar for (a) $D = 0.52$ mm, $L = 100$ mm, (b) $D = 1.1$ mm, $L = 150$ mm, (c) $D = 1.1$ mm, $L = 300$ mm and (d) $D = 1.1$ mm, $L = 450$ mm.

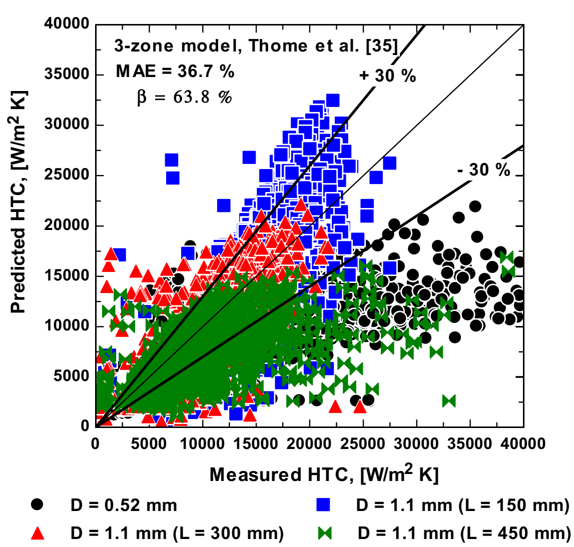

Fig. 7. Global comparison with Thome et al. [35] three zone model.

6. The proposed new correlation

As discussed above, none of the models and correlations could predict the experimental data of all tubes with a reasonable accuracy. The recent statistical correlation proposed by the present authors [31] provided improved predictions for our data. It predicted that the heat transfer coefficient decreases slightly with increasing vapour quality for all tube sizes. As the diameter decreases and/or heated length increases, there is a possibility for the trend of h vs. x to exhibit an increasing trend towards the tube exit. The recent correlation could not predict this increasing trend with quality and therefore it predicted the data of the two longest 1.1 mm tubes (the increasing trend towards the exit was clear in these two tubes) with lower accuracy. The increasing trend of h vs. x towards the tube exit observed in micro tubes may be due to the thinning of the liquid film, the possible suppression of nucleate boiling and the large enhancement in the convective boiling term. Accordingly, to capture the experimental trend, a new additional heat transfer correlation is proposed based on the superposition model of Chen [15], which accounts for the contribution of nucleate and convective boiling. The database used in developing this correlation consists of 5152 data points for R134a and tubes with $D = 4.26$–0.52 mm and includes data obtained previously with the same experimental facility, Huo [50] and Shiferaw [51]. Table 5 includes the parameters and the variables in the data bank and the uncertainties in both the measured and the processed data. This is available to other researchers at (http://www.brunel.ac.uk/sed/mecheng/research/ee/ceber) and should be referenced to this paper.

It is worth mentioning that the data of the 1.1 mm tube with $L = 300$ and 450 mm are excluded. In order to incorporate the effect of heated length into this or any other correlation, a wider range of

Table 4
The statistical assessment of mechanistic models.

Correlation	Diameter/length, mm								All data	
	0.52/100 mm		1.1/150 mm		1.1/300 mm		1.1/450 mm			
	β	MAE	β	MAE	β	MAE	β	MAE	β	MAE
Thome et al. [35]	42	39.2	76	24	75.8	35.7	55	48	63.8	36.7
Consolini-Thome [41]	42.5	41	24.7	40.5	21.3	49.3	10.6	60.8	23.8	48.4

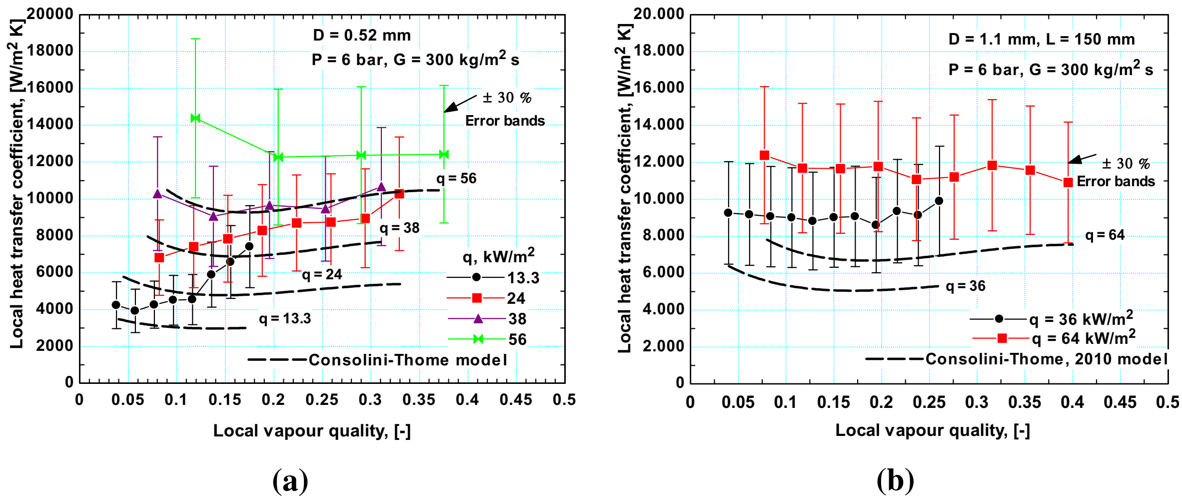

Fig. 8. Comparison with Consolini–Thome [41] model for (a) D = 0.52 mm, L = 100 mm, (b) D = 1.1 mm, L = 150 mm at P = 6 bar and G = 300 kg/m^2 s.

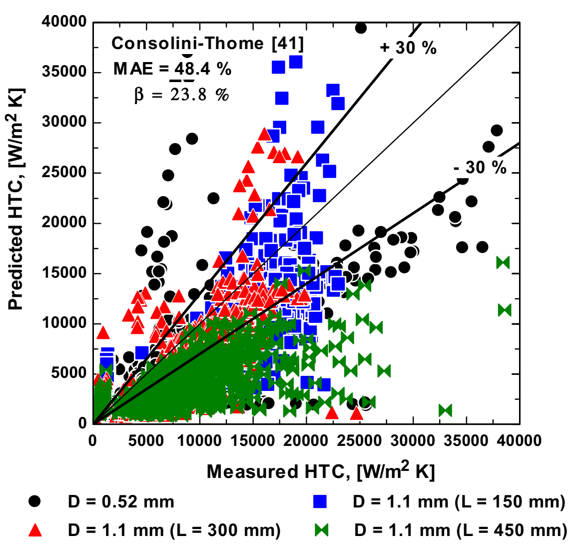

Fig. 9. Global comparison with Consolini and Thome [41] model.

L/D ratios should be studied. The form of the new correlation is given by Eq. (5). Cooper [21] pool boiling correlation given by Eq. (6) is used instead of Forster and Zuber [20] correlation, which was used in the original Chen [15] correlation. The single phase liquid heat transfer coefficient is calculated using the conventional single phase equations for laminar and turbulent flows as given by Eq. (7) based on the liquid Reynolds number defined by Eq. (8). An interpolation was conducted between the laminar and turbulent heat transfer coefficients for the transition region.

$$h_{tp} = S_{new} h_{Cooper} + F_{new} h_L \tag{5}$$

Table 5
The range of experimental parameters in the databank with the uncertainty values.

Parameter	Range (nominal values)	Uncertainty
Mass flux, kg/m^2 s	100–700	±2.2–6%
Fluid inlet temperature, °C	15–50	±0.08 K
Fluid outlet temperature, °C	21–51	
Inlet pressure, bar	6–14	±0.42%
Heat flux, kW/m^2	1.7–158	±0.95–1.95%
Pressure drop, bar	0.005–0.36	±0.07%
Outer wall temperature, °C	20–245	±0.22 K
Heat transfer coefficient, W/m^2 K	854–50000	±3.6–13.7%
Diameter, mm	4.26–0.52	±1.1–3%

$$h_{Cooper} = 55 P_r^{0.12-0.434\ln R_p} (-\log P_r)^{-0.55} M^{-0.5} q^{0.67} \tag{6}$$

$$h_L = \begin{cases} 4.36\frac{k_L}{D} & \mathrm{Re}_L < 2000 \\ 0.023\mathrm{Re}_L^{0.8}\mathrm{Pr}_L^{0.4}\frac{k_L}{D} & \mathrm{Re}_L > 3000 \end{cases} \tag{7}$$

$$\mathrm{Re}_L = \frac{(1-x)GD}{\mu_L} \tag{8}$$

The remaining unknowns in Eq. (5) are the nucleate boiling suppression factor S_{new} and the convective boiling enhancement factor F_{new}. Chen [15] determined these two parameters empirically using experimental data for convective boiling of water and hydrocarbons in large diameter tubes. Therefore, it is no surprise that the correlations proposed by Chen [15] for these two parameters are not expected to work properly with refrigerants in small to micro tubes and consequently new relations are required. The experimental values of the enhancement factor should be determined first in order to propose a new correlation for the enhancement factor F_{new}. Chen [15] proposed two approaches to determine this factor from the experimental data. The first approach involved an iteration process and the second was theoretical based on the analogy between heat and momentum transfer in the boundary layer. Chen [15] did not find any significant difference between the values of the enhancement factors calculated using the two methods. Therefore, in the current study, the second approach was selected to determine the experimental values of the enhancement factor. Chen [15] using this second approach, deduced the enhancement factor theoretically and introduced it as a function of the two phase frictional multiplier:

$$F = (\phi_L^2)^{0.444} \tag{9}$$

Eq. (9) is valid as long as the value of the liquid Prandtl number is about one. Bennet and Chen [52] modified Eq. (9) to extend the Prandtl number range to values greater than one as cited in Collier and Thome [53], given as Eq. (10) below:

$$F = \left[\left(\frac{\mathrm{Pr}_L + 1}{2}\right)\phi_L^2\right]^{0.444} \tag{10}$$

The two phase frictional multiplier proposed by Mishima and Hibiki [54] (see Eq. (11)) was used in this study since it was developed for small to mini diameter tubes and was useful in predicting the current experimental pressure drop data well, see Mahmoud et al. [55]. The determined enhancement factor F_{new} was plotted against the reciprocal of the Martinelli parameter given by Eq. (12), see Fig. 10. A total of 1249 data points for the shortest 1.1 mm diameter tube covering system pressure range of 6–10 bar, mass flux range of 100–500 kg/m^2 s and x up to 0.6–0.8 were used in this figure. It is obvious that, all data points collapsed into one single line without any scatter, which confirms the success of the reciprocal of the Martinelli parameter to correlate the enhancement factor. It is interesting to note that, the trend for the other tubes was similar to that in Fig. 10 but the slope of the curve was found to be dependent on the tube diameter. Therefore, all the data in the current data bank the data for D = 4.26–0.52 mm tube were included in the analysis to correlate the effect of diameter on the new enhancement factor (except the data for D = 1.01 mm and L = 300 and 450 mm). The proposed function for the enhancement factor that was found to fit all the experimental data is given by Eq. (13).

$$\phi_L^2 = 1 + \frac{C}{\mathrm{X}} + \frac{1}{\mathrm{X}^2}, \quad C = 21\left(1 - e^{0.319D}\right) \tag{11}$$

$$\mathrm{X} = \left(\frac{f_L}{f_g}\right)^{0.5}\left(\frac{\rho_g}{\rho_L}\right)^{0.5}\left(\frac{1-x}{x}\right) \tag{12}$$

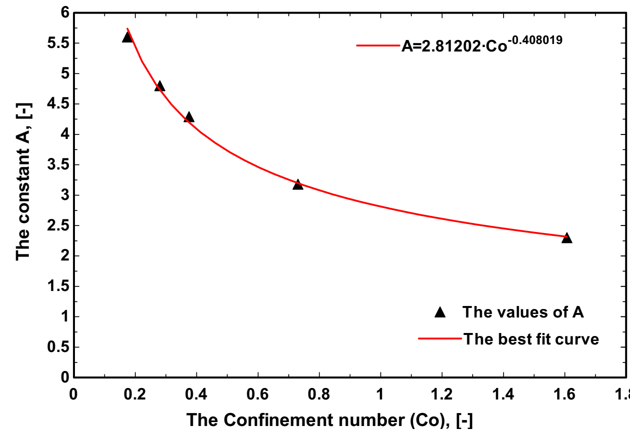

Fig. 11. The constant A in Eq. (11) as a function of the confinement number.

$$F_{new} = \left(1 + \frac{A}{\mathrm{X}}\right)^{0.64} \tag{13}$$

The constant A in the above equation was found to depend strongly on the confinement number as shown in Fig. 11 and was fitted by Eq. (14).

$$A = 2.812Co^{-0.408} \tag{14}$$

As the confinement number increases (diameter decreases), the value of A decreases and consequently the enhancement factor. This may be attributed to the damping of turbulence with decreasing diameter, which reduces the convective heat transfer. This does not contradict with Karayiannis et al. [48] and Consolini and Thome [49] who reported that the flow boiling heat transfer coefficient increases as the diameter decreases. This is because they refer to the average heat transfer coefficient versus heat flux. Reducing tube diameter (increasing confinement number) may significantly increase the nucleate boiling heat transfer coefficient in the low vapour quality region and make the total average value larger.

Fig. 12 depicts a comparison between the new proposed enhancement factor and the original one proposed by Chen [15]. It is obvious that, the two curves approach a value of one as 1/X decreases, i.e. as the vapour quality decreases. This is consistent with the fact that bubbly flow dominates at small vapour quality values and consequently nucleate boiling dominates over convective boiling and hence the enhancement factor should be one. On the other

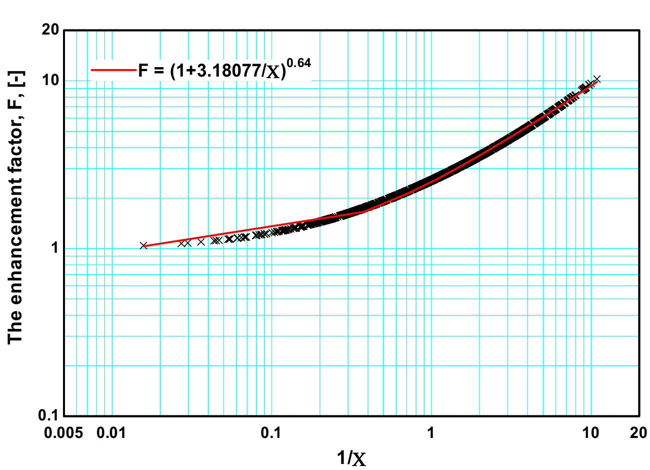

Fig. 10. The experimental enhancement factor versus the reciprocal of Martinelli's parameter.

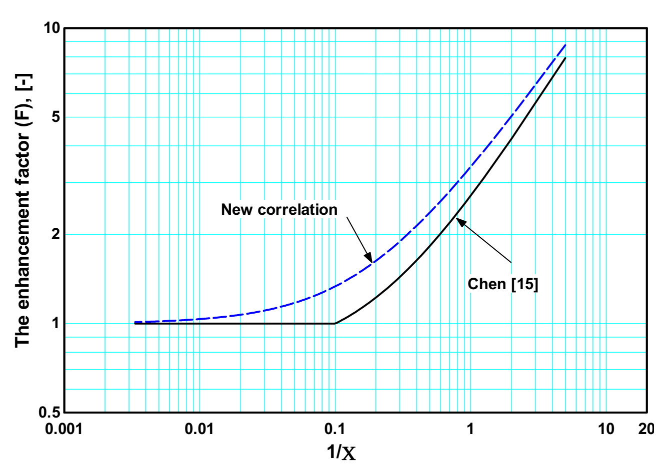

Fig. 12. Comparison between the new enhancement factor and the enhancement factor proposed by Chen [15].

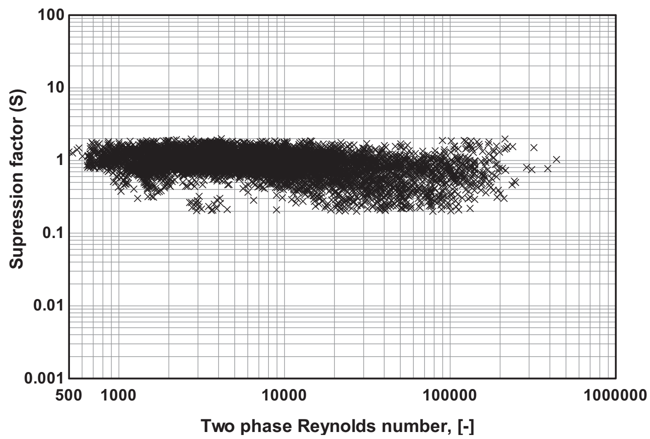

Fig. 13. The experimental suppression factor versus the two phase Reynolds number.

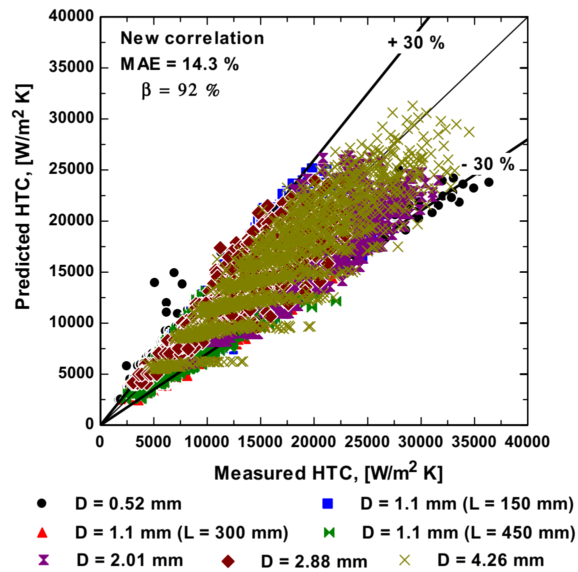

Fig. 15. Global comparison with the new correlation.

hand, the two curves tend to merge at very high values of 1/X. Significant deviations are observed for values between about 0.01 and 2. It is worth mentioning here that Chen [15] used the Martinelli parameter for turbulent liquid and turbulent vapour. In the current study the Martinelli parameter was calculated based on the actual flow conditions, i.e. laminar or turbulent.

The experimental suppression factor was calculated based on the enhancement factor determined using Eq. (15). The result is plotted against the two phase Reynolds number defined by Eq. (16) for all tubes included in our data bank (except D = 1.1 mm and L = 300 and 450 mm), see Fig. 13. The same function proposed by Chen [15] was used to correlate the data in this figure, but modified by the new enhancement factor as given by Eq. (17).

$$S_{Exp} = \frac{h_{tp,Exp} - F_{new} h_L}{h_{Cooper}} \tag{15}$$

$$\mathrm{Re}_{tp} = \mathrm{Re}_L F_{new}^{1.25} \tag{16}$$

$$S_{new} = \frac{1}{1 + 2.56 \times 10^{-6} \left(\mathrm{Re}_L F_{new}^{1.25}\right)^{1.17}} \tag{17}$$

Fig. 14 depicts a comparison between the new suppression factor and the original one proposed by Chen [15]. This figure explains why the original Chen correlation highly under-predicts the current experimental data as previously presented in Fig. 1(a). The figure indicates that the nucleate boiling suppression factor of Chen decreases rapidly with the two phase Reynolds number. This makes the nucleate boiling term in the original correlation very small and consequently the total value of the heat transfer coefficient. On the contrary, the new modified suppression factor remains equal to one up to Reynolds number value of about 5×10^4 then it decreases slowly with increasing Reynolds number.

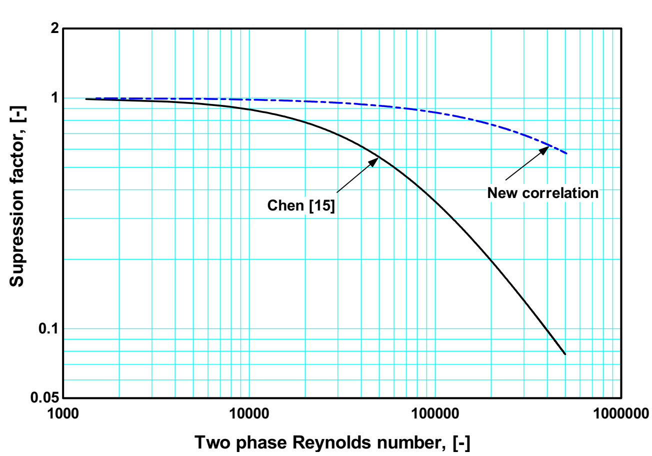

Fig. 14. Comparison between the new correlation of the nucleate boiling suppression factor and the original one proposed by Chen [15].

The new correlation is valid for R134a, D = 4.26–0.52 mm, G = 100–500 kg/m^2 s, P = 6–14 bar and $x < x_{dryout}$, i.e. the correlation is valid as long as there is no dryout. Dryout occurs at approximately x = 0.51, 0.42, 0.41, 0.77, 0.9 for D = 4.26, 2.88, 2.01, 1.1, 0.52 respectively. We expect these dryout values to be a guide but should be verified when using other data to compare with this correlation. Fig. 15 depicts the global comparison between the new correlation and the current experimental data. The correlation predicted 92% of all data within the error bands at a MAE value of 14.3%. It is worth mentioning that the new correlation predicted 93.3% of the data of the 1.1 mm tube (L = 300 mm) at a MAE value of 14% and predicted 87.4% of the longest tube (L = 450 mm) at a MAE value of 16.5%. This means that the performance of the new correlation changes slightly with the variation of the heated length which is different compared to the performance of the examined past correlations including the recent correlation proposed by the present authors.

7. Conclusions

This paper presented a detailed assessment for nineteen correlations as well as two existing mechanistic models. The assessment was conducted using local and average (global) heat transfer coefficients. In summary, our comparison demonstrated that all examined correlations are not general enough and/or could not predict the current experimental data with a reasonable accuracy. Also, the mechanistic models failed to predict the current experimental data of all tubes, which may be attributed to the fact that these models are not totally based on theory but depend on empirical parameters, i.e. they are semi-mechanistic models. A correlation developed earlier by the same authors predicted the current data with a very reasonable accuracy. This was a statistical determined relation, which did not predict the increasing trend of h *vs.* x in micro diameter tubes. However, this gives a very good prediction compared to the other models we examined and can be used in a lot of cases due its ease of application. The performance of most correlations changed with the change of diameter and heated length. This may be due to the fact that most microscale correlations were developed based on channels of short lengths. If the length is too short, the applied heat flux must be much higher for the same exit quality compared to long channels. Accordingly, there is a possibility for the nucleate boiling mechanism to dominate, i.e. the local heat transfer coefficient does not vary with local quality. Therefore, it is expected that these correlations perform poorly as the heated length increases, i.e. as h increases with x towards the channel exit. A new correlation of the Chen type was proposed in this paper, which is more general especially for refrigerants and can predict local and hence average heat transfer coefficient values. The new correlation predicts the increasing trend of h *vs.* x that was observed in micro tubes. The correlation predicted 92% of all data within the ±30% error bands at a MAE value of 14.3%. The new correlation predicted satisfactorily the data for the three different lengths available for the 1.1 mm dia. tube. However, the effect of heated length need to be examined further and included in a future version probably as a non-dimensional term (L/D).

Appendix A. Heat transfer correlations

See Tables A1 and A2.

References

[1] B. Watel, Review of saturated flow boiling in small passages of compact heat exchangers, Int. J. Therm. Sci. 42 (2003) 107–140.
[2] G. Ribatski, W. Zhang, L. Consolini, J. Xu, J.R. Thome, On the prediction of heat transfer in microscale flow boiling, Heat Transfer Eng. 28 (10) (2007) 842–851.
[3] Z.Y. Bao, D.F. Fletcher, B.S. Haynes, Flow boiling heat transfer of Freon R11 and HCFC123 in narrow passages, Int. J. Heat Mass Transfer 43 (2000) 3347–3358.
[4] G.R. Warrier, V.K. Dhir, L.A. Momoda, Heat transfer and pressure drop in narrow rectangular channels, Exp. Therm. Fluid Sci. 26 (2002) 53–64.
[5] R. Yun, J. Hyeok-Heo, Y. Kim, Evaporative heat transfer and pressure drop of R410A in microchannels, Int. J. Refrig. 29 (1) (2006) 92–100.
[6] G. Ribatski, L. Wojtan, J.R. Thome, An analysis of experimental data and prediction methods for two-phase frictional pressure drop and flow boiling heat transfer in micro-scale channels, Exp. Therm. Fluid Sci. 31 (2006) 1–19.
[7] C. Martin-Callizo, R. Ali, B. Palm, New experimental results on flow boiling of R134a in a vertical microchannel, in: UK Heat Transfer Conference, Edinburgh, 10–11 September 2007.
[8] D. Shiferaw, X. Huo, T.G. Karayiannis, D.B.R. Kenning, Examination of heat transfer correlations and a model for flow boiling of R134a in small diameter tubes, Int. J. Heat Mass Transfer 50 (2007) 5177–5193.
[9] F. Xiande, S. Rongrong, Z. Zhanru, Correlations of flow boiling heat transfer of R134a in minichannels: comparative study, Energy Sci. Technol. 1 (1) (2011) 1–15.
[10] Y. Wang, K. Sefiane, S. Harmand, Flow boiling in high aspect ratio mini and micro channels with FC72 and ethanol: experimental results and heat transfer correlation assessments, Exp. Therm. Fluid Sci. 36 (2012) 93–106.
[11] S.S. Bertsch, E.G. Groll, S.V. Garimella, Review and comparative analysis of studies on saturated flow boiling in small channels, Nanoscale Microscale Thermophys. Eng. 12 (3) (2008) 187–227.
[12] H.J. Lee, S.Y. Lee, Heat transfer correlation for boiling flows in small rectangular horizontal channels with low aspect ratios, Int. J. Multiph. Flow 27 (2001) 2043–2062.
[13] W. Qu, I. Mudawar, Flow boiling heat transfer in two phase microchannel heat sinks I: experimental investigation and assessment of correlation methods, Int. J. Heat Mass Transfer 46 (2003) 2755–2771.
[14] T.G. Karayiannis, M.M. Mahmoud, D.B.R. Kenning, A study of discrepancies in flow boiling results in small to micro diameter metallic tubes, Exp. Therm. Fluid Sci. 36 (2012) 126–142.
[15] J.C. Chen, A correlation for boiling heat transfer to saturated fluids in convective flow, Ind. Eng. Chem. 5 (1966) 322–329.
[16] W. Zhang, T. Hibiki, K. Mishima, Correlation for flow boiling heat transfer in mini-channels, Int. J. Heat Mass Transfer 47 (2004) 5749–5763.
[17] S. Saitoh, H. Daiguji, E. Hihara, Correlation for boiling heat transfer of R134a in horizontal tubes including effect of tube diameter, Int. J. Heat Mass Transfer 50 (2007) 5215–5225.
[18] S.S. Bertsch, E.A. Groll, S.V. Garimella, A composite heat transfer correlation for saturated flow boiling in small channels, Int. J. Heat Mass Transfer 52 (7–8) (2009) 2110–2118.
[19] K. Stephan, M. Abdelsalam, Heat transfer correlations for natural convection boiling, Int. J. Heat Mass Transfer 23 (1980) 73–87.
[20] H.K. Forster, N. Zuber, Dynamics of vapour bubbles and boiling heat transfer, Am. Inst. Chem. Eng. J. 1 (1955) 531–535.
[21] M.G. Cooper, Saturated nucleate pool boiling – a simple correlation, in: First UK National Heat Transfer Conference, IChemE Symposium, Series 86, vol. 2, 1984, pp. 785–793.
[22] P.A. Kew, K. Cornwell, Correlations for the prediction of boiling heat transfer in small diameter channels, Appl. Therm. Eng. 17 (8-10) (1997) 705–715.
[23] S.G. Kandlikar, P. Balasubramanian, An extension of the flow boiling correlation to transition, laminar, and deep laminar flows in minichannels and microchannels, Heat Transfer Eng. 25 (3) (2004) 86–93.
[24] D.A. Mikielewicz, A new method for determination of flow boiling heat transfer coefficient in conventional-diameter channels and minichannels, Heat Transfer Eng. 31 (4) (2010) 276–287.
[25] S.G. Kandlikar, A general correlation for saturated two-phase flow boiling heat transfer inside horizontal and vertical tubes, J. Heat Transfer Trans. ASME 112 (1990) 219–228.
[26] H. Muller-Steinhagen, K. Heck, A simple friction pressure drop correlation for two-phase flow in pipes, Proc. Chem. Eng. 20 (1986) 297–308.
[27] G.M. Lazarek, S.H. Black, Evaporative heat transfer, pressure drop and critical heat flux in a small vertical tube with R-113, Int. J. Heat Mass Transfer 25 (7) (1982) 945–960.
[28] T.N. Tran, M.W. Wambsganss, D.M. France, Small circular- and rectangular-channel boiling with two refrigerants, Int. J. Multiph. Flow 22 (3) (1996) 485–498.
[29] J. Lee, I. Mudawar, Two-phase flow in high heat flux microchannel heat sink for refrigeration cooling applications. Part II: Heat transfer characteristics, Int. J. Heat Mass Transfer 48 (2005) 941–955.
[30] W. Li, Z. Wu, A general correlation for evaporative heat transfer in micro/mini-channels, Int. J. Heat Mass Transfer 53 (2010) 1778–1787.
[31] M.M. Mahmoud, T.G. Karayiannis, A statistical correlation for flow boiling heat transfer in micro tubes, in: Proceedings of the Third European Conference on Microfluidics–Microfluidics 2012, Springer, Heidelberg, 2012, pp. 3–5 (December).
[32] Z. Liu, R.H.S. Winterton, A general correlation for saturated and subcooled flow boiling in tubes and annuli, based on a nucleate pool boiling equation, Int. J. Heat Mass Transfer 34 (11) (1991) 2759–2766.
[33] T.N. Tran, M.W. Wambsganss, M.-C. Chyu, D.M. France, A correlation for nucleate flow boiling in small channels, in: Compact Heat Exchangers for the Process Industries Conference, Snowbird, Utah, June 22 – 27, 1997.
[34] A.M. Jacobi, J.R. Thome, Heat transfer model for evaporation of elongated bubble flows in microchannels, J. Heat Transfer 124 (6) (2002) 1131–1136.
[35] J.R. Thome, V. Dupont, A.M. Jacobi, Heat transfer model for evaporation in microchannels. Part I: Presentation of the model, Int. J. Heat Mass Transfer 47 (2004) 3375–3385.
[36] K. Moriyama, A. Inoue, Thickness of the liquid film formed by a growing bubble in a narrow gap between two horizontal plates, J. Heat Transfer 118 (1996) 132–139.
[37] V. Dupont, J.R. Thome, A.M. Jacobi, Heat transfer model for evaporation in microchannels. Part II: Comparison with the database, Int. J. Heat Mass Transfer 47 (2004) 3387–3401.
[38] D. Shiferaw, T.G. Karayiannis, D.B.R. Kenning, Flow boiling in a 1.1 mm tube with R134a: experimental results and a comparison with model, Int. J. Therm. Sci. 48 (2009) 331–341.
[39] W. Qu, I. Mudawar, Flow boiling heat transfer in two phase microchannel heat sinks – II. Annular two phase flow model, Int. J. Heat Mass Transfer 46 (2003) 2773–2784.
[40] H. Boye, Y. Staate, J. Schmidt, Experimental investigation and modelling of heat transfer during convective boiling in a minichannel, Int. J. Heat Mass Transfer 50 (2007) 208–215.
[41] L. Consolini, J.R. Thome, A heat transfer model for evaporation of coalescing bubbles in micro-channel flow, Int. J. Heat Fluid Flow 31 (1) (2010) 115–125.
[42] X. Huo, Y.S. Tian, T.G. Karayiannis, R134a Flow boiling heat transfer in small diameter tubes, in: Advances in Compact Heat Exchangers, R.T. Edwards, Inc., 2007, pp. 95–111 (Chapter 5).
[43] M.M. Mahmoud, T.G. Karayiannis, D.B.R. Kenning, Surface effects in flow boiling of R134a in microtubes, Int. J. Heat Mass Transfer 54 (2011) 3334–3346.
[44] M.M. Mahmoud, D.B.R. Kenning, T.G. Karayiannis, Single and two phase heat transfer and pressure drop in a 0.52 mm vertical metallic tube, in: Seventh International Conference on Enhanced, Compact and Ultra-Compact Heat Exchangers: From Microscale Phenomena to Industrial Applications, Heredia, Costa Rica, 13–18 September, 2009.
[45] M.M. Shah, Chart correlation for saturated boiling heat transfer: equations and further study, ASHRAE Trans. 88 (pt 1) (1982) 185–196.
[46] K.E. Gungor, R.H.S. Winterton, A general correlation for flow boiling in tubes and annuli, Int. J. Heat Mass Transfer 29 (1986) 351–358.
[47] O. Steiner, J. Taborek, Flow boiling heat transfer in vertical tubes correlated by an asymptotic model, Heat Transfer Eng. 13 (2) (1992) 43–69.
[48] T.G. Karayiannis, D. Shiferaw, D.B.R. Kenning, Flow boiling in small- to micro-diameter tubes: experimental results and modelling, in: ECI International Conference on Heat Transfer and Fluid Flow in Microscale, Whistler, September 2008, pp. 21–26.
[49] L. Consolini, J.R. Thome, Micro-channel flow boiling heat transfer of R-134a, R-236fa, and R-245fa, Microfluid. Nanofluid. 6 (6) (2009) 731–746.

[50] X. Huo, Experimental study of boiling heat transfer in small diameter tubes, Ph.D. Thesis, London South Bank University, London, UK, 2005.
[51] D. Shiferaw, Two phase flow boiling in small- to micro-diameter tubes, Ph.D. Thesis, Brunel University, UK, 2008.
[52] D.L. Bennet, J.C. Chen, Forced convection boiling in forced tubes for saturated pure fluids and binary mixtures, Am. Inst. Chem. Eng. J. 26 (3) (1980) 454–464.
[53] J.G. Collier, J.R. Thome, Convective Boiling and Condensation, third ed., Oxford University Press, Oxford, UK, 1994.
[54] K. Mishima, T. Hibiki, Some characteristics of air–water two-phase flow in small diameter vertical tubes, Int. J. Multiph. Flow 22 (4) (1996) 703–712.
[55] M.M. Mahmoud, T.G. Karayiannis, D.B.R. Kenning, Flow boiling pressure drop of R134a in micro diameter tubes: experimental results and assessment of correlations, in: Third Micro and Nano Flows Conference, Thessaloniki, Greece, 22–24 August 2011.